Effect of Seashell Waste on Thermal and Mechanical Properties of High Strength Concrete

A Thesis of

Master of Science

By

Muhammad Hamza Ahsan

(NUST-2018-MS SE 00000275465)

December 2021

Department of Structural Engineering

Military College of Engineering, Risalpur

National University of Science & Technology

Islamabad, Pakistan

(2021)

THESIS ACCEPTANCE CERTIFICATE

This is to certify that the

thesis titled

Effect of Seashell Waste on Thermal and Mechanical Properties of High Strength Concrete

Submitted by

Muhammad Hamza Ahsan

(00000275465)

has been accepted towards the partial fulfillment

of the requirements for the degree of

Master of Science in Structural Engineering

_____

Dr. Muhammad Shahid Siddique

Assistant Professor,

Department of Strutural Engineering,

Military College of Engineering, Risalpur

National University of Sciences and Technology (NUST), Islamabad

DECLARATION

I certify that this research work titled "**Effect of Seashell Waste on Thermal and Mechanical Properties of High Strength Concrete***"* is my own work. The work has not been presented elsewhere for assessment. The material that has been used from other sources it has been properly acknowledged / referred.

_____

Signature of Student

Muhammad Hamza Ahsan

(2018-NUST-MS SE-00000275465)

This thesis is dedicated to my family.

ACKNOWLEDGEMENTS

Firstly I would like to thank Allah for helping me to get through and blessing me with the patience and success to reach where I am today.

I am grateful to my Supervisor **Dr. Muhammad Shahid Siddique** for his sincere help. I am also thankful to my GEC members **Dr. Syed Hassan Farooq** and **Dr. Muhammad Rizwan** for their never ending help and mentoring at every stage of this research. Without their guidance and motivation, this research would have never been possible. I am also very thankful to my friends **Engr. Ashar**, **Engr. Haziq**, **Engr. Huzaifa**, **Engr. Israr**, **Engr. Zeeshan**, **Engr. Zia**, **Engr. Junaid**, **Engr. Abdul Rehman** and **Engr. Husnain** for always being there for me in this journey.

Last but not the least, I am grateful to my family members, without their prayers and support, I would have never achieved anything.

ABSTRACT

Seashells are one of the numerous wastes that are quickly accumulating onshore coasts on the Arabian Sea, Karachi, Pakistan causing pollution for the environment. The seashell (SS) waste that causes various diseases and hazardous for environment can be used in concrete (0, 10, 20, and 30%) and in plastering mortar (20%, 40% and 60%) in place of fine aggregate to create an eco-friendly high strength concrete (HSC). Concrete materials undergo higher temperatures during their service period due to fire. After exposure to fire, properties of concrete have a prime importance in terms of serviceability of buildings and occupants' safety. Therefore, to improve the fire resistant of high strength concrete, seashell waste was included, which is possibly a thermal degradable fiber. The mechanical properties namely compressive strength, stress-strain response, elastic modulus, compressive toughness, strain ductility and mass loss of modified and controlled samples, as well as the deterioration caused by elevated temperatures exposure were studied. The analyzed formulations were heated to a temperature of 200, 400, 600, and 800°C at a heating rate of 5°C/min and then tested for residual conditions. Seashell modified samples showed a higher compressive strength, elastic modulus, compressive toughness as compared to control sample at elevated temperature with less spalling sensitivity. According to visual inspection, SS-HSC as compared to HSC showed less cracking at higher temperatures. Moreover, the effect of plastering high strength concrete with seashell showed greater strength with more fire resistant to concrete core. Conclusively, utilization of seashell in high strength concrete is efficient for eco-friendly as well as fire resistant concrete.

TABLE OF CONTENTS

LIST OF FIGURES

LIST OF TABLES

LIST OF ABBREVIATIONS

SS	Seashell
HSC	High Strength Concrete
NSC	Normal Strength Concrete
SRMs	Secondary Raw Materials
HRWRs	High Range Water Reducers
SS-HSC	Seashell High Strength Concrete
SP-HSC	Seashell Plaster High Strength Concrete
PPF	Polypropylene Fibers
HSLWC	High Strength Light Weight Concrete
LWC	Light Weight Concrete
LFC	Light Foamed Concrete
LWA	Light Weight Aggregate
CSS	Crushed Seashell
SCMs	Self-Compacting Mortars
GGBFS	Ground Granulated Blast Furnace Slag
NS	Nano silica
SF	Silica Fume
FA	Fly Ash
TC	Thermocouples
LVDTs	Linear Variable Displacement Transducers

CHAPTER 1

INTRODUCTION

1.1 General

Concrete is a widely used construction material. Its widespread usage is mainly due to its versatility derived from ease of forming into any shape and ease of production using locally available materials and relatively unskilled labor. The concrete structure is subjected to various types of loading during their life span which includes dead, live, wind and impact and also in some severe cases environmental hazards like earthquake loading and fire exposure etc. Therefore in concrete technology durability of concrete has given a prime importance. The behavior of concrete mostly depends on the properties of materials used, proportioning of its ingredients, chemical and physical characteristics of materials and curing conditions etc. Under normal condition, concrete structures are subjected to wide range of temperatures which is not very harsh for concrete material properties. Fire, on the other hand, is always a threat to civil engineering structures since it is one of the most severe and unpredictable risks that can impact the functioning of a structural system over its lifetime. It claims thousands of lives each year and causes billions of dollars in property damage on a global scale (Evart 2018). Therefore, it becomes essential to have the understanding of fire impact on the material and chemical properties of concrete to design structure capable of withstanding the elevated temperatures as occurs in the incident of fire. Concrete exposure to fire can cause serious deleterious effects on concrete.

Concrete subjected to high temperatures (over 200°C) from an accidental fire or excessive heat from industrial plants causes cracks and damages the building due to high internal tensile stresses (Al-Akhras, Al-Akhras et al. 2009). These high temperatures causes some defects in concrete structures namely cement paste dehydration, reduction in compressive and tensile strength, loss in mass, increase in permeability and porosity, creep and expansion, and spalling in extreme cases (Bažant, Kaplan et al. 1996, Noumowé, Siddique et al. 2009). Exposure of concrete to higher temperatures can affect its thermal, mechanical, deformation, material and physical properties. The behavior of high strength concrete (HSC) is peculiar as compare to normal strength concrete on elevated temperature.

Fabrication of HSC requires a deep understanding of the knowledge of the usage of water reducers, super plasticizers, pozzolans, secondary raw materials (SRMs) etc. Production and usage of HSC opened the new paths in the construction industry and concrete technology and is widely used all over the world. Although HSC is a significant improvement in the concrete industry, several experimental tests have found that HSC members have lesser fire resistance than NSC members (Lie and Woollerton 1988, Kodur, Khaliq et al. 2013). HSC members have a lower high-temperature performance because of rapid strength deterioration and fire-induced spalling (Khaliq and Kodur 2011, Khaliq 2012).

Seashells are just one of the many wastes that are rapidly accumulating along shorelines. Use such material as a replacement of sand in this study is to check the mechanical behavior of high strength concrete. This study was also designed to look into the usage of seashell (as a replacement of sand) as a low-cost, readily available alternative to non-renewable resources in mortars in order to possibly improve their fire resistance.

1.2 Seashell waste concrete and mortar

Concrete is exposed to high temperatures during fires or near furnaces and reactors (Sakr and El-Hakim 2005). These exposures can decrease in mechanical properties like elastic modulus, strength, and volume stability to deteriorate, resulting in structural failures. Exposure to high temperatures also changes the appearance of its surface significantly.

The use of finely ground wastes or by-products in concrete has grown increasingly popular since it can produce better results and more successfully, particularly in terms of the material's mechanical properties and durability. Several waste kinds have been mentioned in the literature, such as fly ash for making Portland cement with additives (Duval and Kadri 1998, Poon, Lam et al. 2000, Barnett, Soutsos et al. 2004, Mazloom, Ramezanianpour et al. 2004, Toutanji, Delatte et al. 2004), or powdered granulated blast furnace slag as a concrete additive (Bijen 1996, Miura and Iwaki 2000, Toutanji, Delatte et al. 2004, Safi, Benmounah et al. 2011, Safi, Ghernouti et al. 2013). Other trash or byproducts with particle sizes greater than cement can be utilized as aggregates in mortar or concrete. Plastic wastes, glass wastes, shattered brick, and demolition debris are all examples (Shi and Zheng 2007, Naceri and Hamina 2009, Demir, Yaprak et al. 2011, Pašalić, Vučetić et al. 2012, Safi, Saidi et al. 2013). (Safi, Saidi et al. 2013) recently reported on the use of plastic wastes as a fine aggregate in mortar.

In comparison to other insulation materials, seashell has the unique ability to improve the thermo-physical properties of concrete at a significantly lower cost. According to (Lertwattanaruk, Makul et al. 2012), increasing the amount of ground seashell replacement decreased the thermal conductivity of the mortars.

The use of seashell in high strength concrete should be researched because of the possible benefits of seashell concrete, such as sustainability and thermal efficiency. In addition, the fire resistance of seashells must be tested in mortar. Likewise, there is no consideration of the thermal and mechanical performance of seashell high strength concrete in elevated temperatures/fire conditions in the literature. As a result, the current study is an attempt to address the issues raised.

1.3 High strength concrete (HSC)

HSC stands for high-strength concrete, which means it has a higher compressive strength than regular or standard concrete. The difference in their 28-day compressive strength is the main distinction between HSC and NSC. Among standards and writers, the threshold strength value that distinguishes between HSC and NSC is unclear. The value of this threshold varies between publications and standards. HSC is defined by (Committee 2008) as concrete with a compressive strength higher than 41.25 MPa (6000 psi). In this study, the strength barrier set by (Committee 2008) is regarded the lowest strength of HSC.

To manufacture HSC, two different chemical compositions are added to improve the mechanical properties of traditional concrete, such as compressive strength. Water reducers, also known as high-range water reducers or SRMs, are two types of SRMs. While lowering the w/c of concrete improves its compressive strength, it also reduces its workability, which is defined as the "ease with which the concrete may be handled, mixed, or put" (A. 2013). Because of this loss, concrete installation and consolidation are almost impossible, resulting in enormous voids of entrapped air and a reduction in hardened concrete strength. High range water reducers (HRWRs) are added to concrete during the mixing phases to produce effective workability at very low water to cement ratios. Mineral admixtures (natural or artificial), often known as SRMs or supplementary cementitious materials, or simply pozzolans, are another type of chemical admixture.

(Committee 2008) characterized SRMs as "a siliceous and aluminous material that has little or no cementitious value in isolation but will chemically react with finely divided calcium hydroxide in the presence of moisture at normal temperatures to produce cementitious compounds." The mechanical strength of concrete can be significantly boosted by using these two chemical compositions, namely water reducers and supplemental raw materials.

1.4 Fire behavior of high strength concrete

The performance of NSC under fire is excellent, as all researches agree. NSC has a lower strength loss (compressive and tensile), a lower mass loss, a lower stress-strain modulus, and a lower probability of spalling after a fire. Because of this tendency, concrete is utilized in a large number of structures that are exposed to fire. When a fire occurs, concrete structures provide ample and acceptable time for inhabitants to evacuate as well as fire fighters to mitigate the flames. All of this is true, however, for standard strength concrete with pores that have hardened due to the increased water content. In contrast to the NSC, the HSC has quick strength loss, a larger modulus drop, and frequent spalling. Spalling of concrete cover is another very destructive result of fire that is more pronounced in HSC, especially in concrete that includes Silica Fume, as documented by (Sanjayan and Stocks 1993). Porosity decreases when the microstructure of HSC improves. HSC has a lower porosity, which contributes to the explosive spalling phenomenon. The tests conducted by (Zeiml, Leithner et al. 2006) support this explanation. The use of PP fibers improves concrete permeability at temperatures above the melting point of the fibers employed, reducing spalling.

1.5 Problem statement

During the service life of a concrete structure, fire is regarded one of the most serious hazards. Furthermore, due to its superior mechanical and durability performance, the construction sector is rapidly shifting to the usage of high strength concrete (HSC). The thick microstructure of HSC, on the other hand, makes it more vulnerable to fire damage. Landfill scarcity and pollution occur from the production of significant amounts of solid waste materials such as seashell waste. When utilized in concrete, seashell has the ability to produce long-lasting, energy-efficient concrete. This raises the possibility of engineering consideration and the replacement of seashell waste in concrete with a less expensive and readily available material in HSC.

The appropriate use of seashell debris in HSC and mortar (as a concrete plaster) may result in a concrete with refined thermal and mechanical properties, which could lead to improved high strength concrete performance at increasing temperatures.

1.6 Objectives

The primary aim of this research study is to investigate the fire behavior of SS-HSC (seashell high strength concretes) and SP-HSC (seashell plaster high strength concrete) in terms of its material and mechanical properties in the temperature range between 23-800°C. The objectives of the study include:

- To study the mechanical properties of high strength concrete using seashell waste as a replacement of sand.
- To study the effectiveness of seashell mortar in improving the thermal resistance of HSC under elevated temperature.

1.7 Research significance

The effect of increased temperature on the mechanical, microstructure, thermal, and permeability properties of both HSC and NSC is well established, and there is ample test data in the literature. It is necessary to investigate the possible properties of seashell included in high-strength concrete. Although enough test data on the usage of seashell in conventional concrete at ambient circumstances is available in the literature, its ability to increase the fire surviving qualities of high strength concrete (coating and without coating) still needs to be investigated.

1.8 Scope of the study

The scope of the study is to improve fire resistance of HSC by using seashell, which is a low-cost, commercially available alternative to nonrenewable minerals. The post-fire residual properties were investigated since they are the most regularly reported in the literature and hence can be compared correctly. Seashell is used to partially replace sand in the concrete mixes (0%, 10%, 20% and 30% by volume of sand) and in plaster (as a coating of HSC) with different percentages i.e., 20%, 40% and 60% (by volume of sand) respectively. HSC has been made in two strengths: high strength modified (including SS) and control and for coating HSC with modified cement mortar (including seashell). The goal of this research is to evaluate the spalling sensitivity, compressive strength, stress-strain response, elastic modulus, compressive toughness, strain ductility and mass loss of seashell modified samples to that of reference HSC samples.

The evaluated formulations were heated to a target temperature of 200, 400, 600 and 800°C using a controlled heating rate of 5°C/min.

1.9 Research methodology

Flow chart of research methodology is as below:

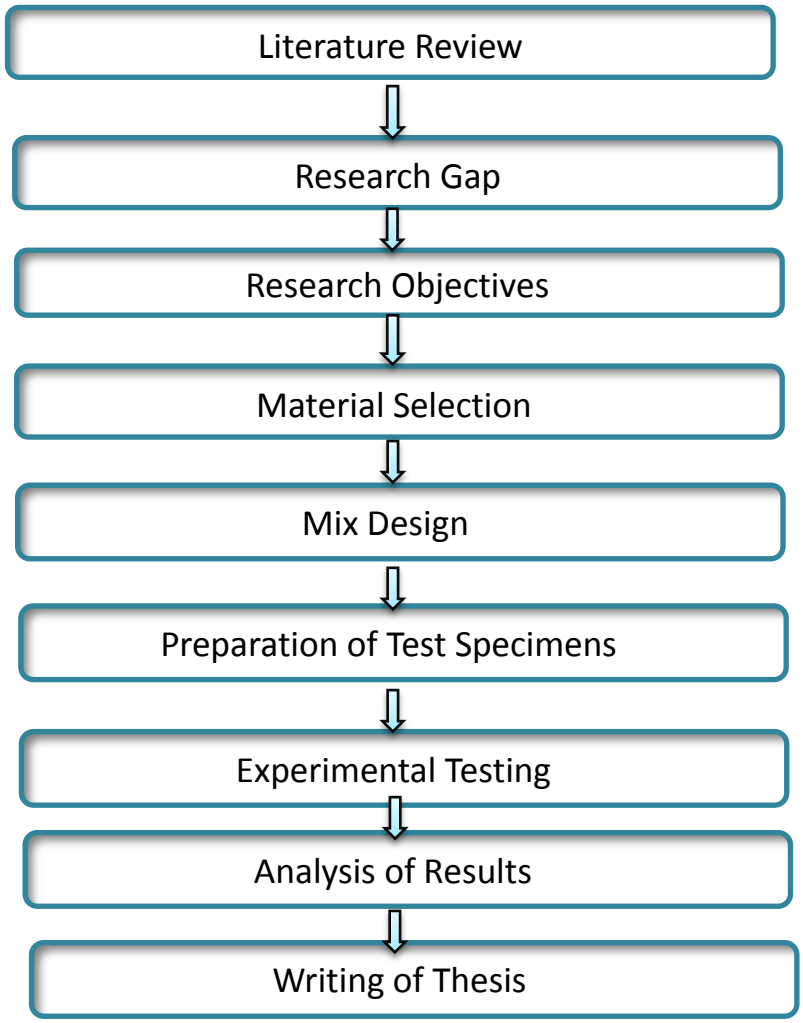

Figure 1.1 Flow chart of research

1.10 Thesis layout

The research undertaken to address the aforementioned objectives is presented in five chapters. Chapter 1 "Introduction" explains the importance of high strength concrete HSC and its behavior under fire, seashell concrete, research objectives, research significance, scope of the study, research methodology, and thesis outline.

Chapter 2 “Literature Review” a brief revision on the previously related researches regarding HSC and the incorporation of seashell in NWC has been presented. The literature review also includes the effect of fire on mechanical properties and spalling of HSC.

Chapter 3 “Experimental program” discusses the test procedures and methodology. The target temperatures, heating rate, specimen size and equipments details of this research study are presented in this chapter.

Chapter 4 “Results and Discussion” includes evaluation, analysis and discussion for results of thermal and material property tests. A result of compressive strength analysis has also been presented.

Chapter 5 “Conclusions and Recommendations” provides the detailed conclusions based on the outcomes of this research and remarks for further studies.

CHAPTER 2

LITERATURE REVEIW

2.1 General

Concrete is now widely used as a construction material in the current period due to its remarkable performance in terms of high compressive strength, higher modulus of elasticity, ease of preparation, water tightness, resistance to corrosive agents, superior fire ratings, and so on. There have been gradual improvements in the properties of concrete since it was first introduced to the construction sector. Concrete's compressive strength is a direct indicator of its performance quality; a concrete with a higher compressive strength has a larger modulus of elasticity, tensile strength, and lower permeability, and thus has a higher durability. The compressive strength of concrete determines the majority of its qualities. With developments in material science, superplasticizers (SP) or high range water reducers (HRWRs) have been used to manufacture concrete with extremely high compressive strength, and the use of HSC has become quite popular. In terms of greater durability and economics, HSC has a lot of advantages. The use of various solid waste materials as replacements for fine aggregates in concrete, such as seashell obtained on seashores as a waste, has become a complementary practice in current construction practice because it results in ecofriendly, sustainable concrete with improved thermal properties. In the case of a fire, HSC structures may be exposed to higher temperatures during their service life. Numerous researches have been conducted on the performance of concrete at high temperatures. The results reveal that, despite its superior performance in all other conditions, HSC performs poorly at elevated temperatures when compared to NSC.

As shown by a global survey of solid waste generation, the rapid expansion in industrialization is leading to rising accretions of diverse industrial wastes. Crushed seashell, a marine byproduct, was most likely used in concrete as a partial substitute for fine aggregate, coarse aggregate, and cement. Few studies have been done on the use of seashells as a partial or complete replacement for fine aggregates (sand) in mortar and concrete production. To address their environmental and economic concerns, effective techniques such as recycling and usage in composite materials are required. The use of seashell in concrete as a replacement for natural fine aggregates (sand) provides an environmentally benign and long-term solution to the problem of seashell disposal, as well as the ability to improve the thermo-mechanical properties of concrete.

Seashell can be used as a partial replacement for fine particles in concrete as well as in mortarA seashell, often known as a sea shell or simply a shell, is a hard, protective outer coating produced by a sea animal. The shell is a part of the animal's body. Beachcombers are frequently come across empty seashells washed up on the shore. The soft parts of the animal have been devoured by another animal or have disintegrated, thus the shells are empty. When seashell (SS) is utilized in concrete and mortar, it provides both concrete and mortar with a low bulk density, improved heat retention, and heat insulating properties.

2.2 Spalling issues in high strength concrete

When concrete structures (particularly HSC) are exposed to rapidly increasing temperatures as seen in fire, spalling is stated to occur when the layers or portions of concrete are observed to break or separate, often with an explosion. Spalling poses the greatest danger to a structure because it exposes the inner layers or core of the concrete structure to fire. This exposure raises the temperature in the concrete core, which is the main load bearing area, and if steel reinforcements are present in the vicinity of thermal exposure, then reinforcement strength begins to deteriorate, the fire resistance of the entire structure decreases rapidly, and the structure eventually collapses due to spalling. Fire-induced spalling is a rare occurrence in NSC. (Sanjayan and Stocks 1993) Measured the weight of the concrete structure with relation to time or temperature (since temperature increased with time) to capture the spalling behavior of HSC and NSC, as illustrated in Figure 2.1.

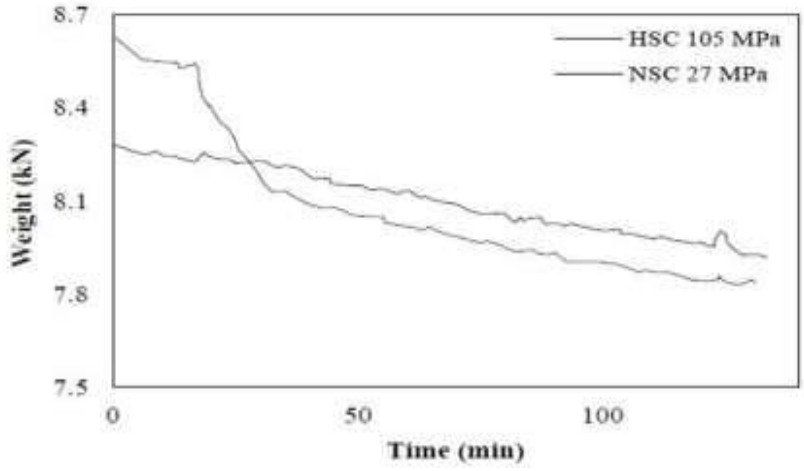

Figure 2.1 Mass loss measured with increasing time and temperature for NSC and HSC (Sanjayan and Stocks 1993)

As seen in Figure 2.1, there is a dramatic decline in weight of the structure after almost 17 minutes, which corresponds to spalling in HSC, demonstrating that HSC is more prone to spalling than NSC. (Phan 2002) found that concrete spalling caused by fire is explosive in character. The investigations on explosive spalling by various authors are listed in Table 2.1. Table 2.1 shows that when HSC is exposed to high temperatures, spalling does not always occur. However, there are some conditions that increase the likelihood of spalling. These variables can be self-contained or interdependent. Table 2.1 shows that the odds of explosive spalling are higher in mixes made with silica fume.

It is vital to have a comprehensive understanding of the causes of concrete spalling in order to prevent it. Prevention is difficult without understanding the mechanism of spalling and its interdependencies. Different mechanisms of spalling have been proposed in the literature. The inconsistency may emerge as a result of the several elements that influence spalling. Furthermore, these variables are interdependent on one another. According to (Kodur 2000), different researchers have proposed two basic theories to explain the spalling activity of HSC. These are:

a) Internal Pore Pressure
b) Release of thermal stresses

2.2.1 Internal pore pressure

When HSC is subjected to fire, the water vapours are unable to find a way to escape from the concrete surface due to its limited permeability. Pore pressure builds up as a result of the impediment caused by the concrete's poor permeability. At 300°C, pressure can reach 8 MPa, which is more than concrete's tensile strength (generally not more than 6 MPa). As a result, chunks of concrete fall off the surface, which, depending on the concrete and fire properties, might be explosive (Anderberg 1997).

Table 2.1 Spalling in concrete at elevated temperatures reported by various authors

SRM Used	**Author**	**Short Name**	**w/c**	**OPC Kg/m3**	**SRM Kg/m3**	**Heating Rate**	**Testing Method**
Fly ash concrete	(Xu et al. 2001)	FAC	0.3	255	275	1°C/min	Unstressed Residual
Silica fume concrete	(Behnood and Ziari 2008)	SFC	0.3	450	45	3°C/min	Unstressed Residual
Metakaolin concrete	(Poon et al. 2003)	MKC	0.3	400	100	2.5°C/min	Unstressed Residual
Blast Furnace	(Siddique and Kaur 200)	SC1	0.45	180	270	8°C/min	Unstressed Residual
Blast Furnace Slag concrete	Xiao et al. 2006	SC2	0.34	261	261	25°C/min	Unstressed Residual
Air entrained concrete	(Khaliq and Farhan 2017)	AEH-4	0.3	500	1077	10°C/min	Unstressed Residual
Recycle aggregate concrete	(Khaliq , Taimur 2018)	RA-HSC	0.32	500	50	10°C/min	Unstressed Residual

2.2.2 Release of thermal stresses

The explanation of spalling due to pore or vapor pressure growth, according to (Kodur 2000), is only a weak point. The actual phenomena that causes explosive concrete spalling is that when a concrete surface is directly exposed to fire, the hotter zone expands, which is restrained by the adjoining concrete, creating thermal strains in the hotter region. The release of stored energy as a result of thermal stresses is the primary cause of explosive spalling. Fracture mechanics must be used to examine this release.

2.3 Various techniques to mitigate fire induced spalling

2.3.1 Role of polypropylene fibers

According to (Kodur 2000), the pore pressure buildup mechanism is merely a trigger for spalling rather than the primary cause. The inclusion of polypropylene fibers in concrete is the most commonly acknowledged and widely utilized approach for preventing spalling from occurring. By maintaining all of the characteristics the same, concrete specimens cast with and without polypropylene fibers (PPF) demonstrate the efficiency of these fibers. (Han, Hwang et al. 2005) conducted similar experiments and found that polypropylene is a very effective technique for dealing with spalling. Table 2.2 summarizes the experimental results data.

Table 2.2 Spalling of concretes with different dosage of PPF

w/cm	**PP Fiber (% of total volume)**	**Specimens**		
		A (Metal fabric)	**B (Glass Fiber)**	**C (Carbon Fiber)**
0.3	0	No Spalling	No Spalling	No Spalling
	0.05	No Spalling	No Spalling	No Spalling
	0.1	No Spalling	No Spalling	No Spalling
0.4	0	No Spalling	No Spalling	No Spalling
	0.05	No Spalling	No Spalling	No Spalling
	0.1	No Spalling	No Spalling	No Spalling

However, due to its fiber length, the use of polypropylene fibers in HSC produces challenges such as non-uniformity in mixing and slump. Furthermore, its disintegration forms a lengthy channel, similar to the pores in concrete, which may contribute to HSC's high-temperature durability concerns.

2.3.2 Role of lightweight aggregates

As a matter of fact high strength lightweight concretes (HSLWC) can be made. These high strength composites can be made in two ways:

- By using mineral admixtures that can show pozzolanic activity like condensed silica fume (CSF), or by using chemical admixtures and specially high-range water reducing admixtures (HRWRA).
- By using high strength, high stiffness lightweight aggregates

LWC has a natural fire resistance. As the temperature rises, typical aggregates expand while the surrounding paste shrinks due to water evaporation, resulting in thermal cracking. This incompatibility is insignificant in the case of LWC constructed of expanded lightweight aggregates. The coefficient of thermal expansion of expanded light weight aggregates is 50 to 70% lower than that of gravel, reducing the probability of light weight concrete expansion to one-fourth(Chandra and Berntsson 2002). Because the vesicular structure of aggregates reduces the thermal conductivity of lightweight mixtures, the calcium silicate hydrate (C-S-H) gel retains its cementitious properties for a long time because the vesicular structure prevents heat from penetrating the core of lightweight concrete samples (Sancak, Sari et al. 2008). An open pore structure allows vapors to escape cementitious matrices, preventing the formation of pore pressure. For the reasons stated above, LWC is one of the finest performing concretes under fire circumstances.

(Felicetti, Gambarova et al. 2013) looked into the thermo-mechanical properties of light-weight concrete (LWC) when it was exposed to high temperatures. He concluded that HPLWC is more temperature-sensitive than LWC or NSC beyond 400°C for compressive strength and throughout the temperature range for stabilized elastic modulus.

(Hora, Štefan et al. 2013) investigated the fire resistance of various reinforced components created with LWC and determined that the fire resistance of horizontal structural members such as slabs and panels made with LWC is lower than that of NWC. Because vertical parts, such as columns, have a lower thermal conductivity, LWC built with expanded clay aggregates have a stronger fire resistance.

LWC's unique thermal properties, such as thermal conductivity, diffusivity, and specific heat, make it an excellent insulator. (Real, Gomes et al. 2016) believes that lightweight concretes have the potential to be employed as an ideal insulating medium after studying the thermal bridging effect and energy performance of structures produced with LWC. The study's findings show a 53 percent decrease in thermal conductivity, a 35 percent increase in specific heat, and a 47 percent decrease in thermal diffusivity. All of these characteristics combine to make light weight concrete (LWC) one of the best fire-resistant and insulating concretes.

(Othuman and Wang 2011) investigated lightweight foamed concrete (LFC) partition walls with densities varying from 600 to 1800 kg/m3. Under typical fire exposure, LFC walls outperform gypsum walls in terms of thermal insulation, making them a cost-effective and practical option for portioning walls.

(Oktay, Yumrutaş et al. 2015) concluded that replacing standard weight aggregates with LWA such as pumice, rubber aggregates, and expanded perlite improves the insulating qualities of modified composites in a study on thermo-physical properties of LWC. Because of the reduction in thermal qualities such as conductivity and diffusivity, lightweight aggregate concretes are not only good insulators but also fire resistant.

Although the use of lightweight aggregates improves the thermal characteristics of concrete at elevated temperatures, light weight aggregates are more difficult to come by than regular weight coarse aggregates for use in concrete. Natural elements such as clay, shale, slate, perlite, and vermiculite are used in a thermal process to create lightweight aggregates.

2.4 Thermal and mechanical properties of seashell in concrete and mortar

The researchers used a variety of strategies to improve the thermal insulating qualities of concrete by using both industrial and agricultural leftovers. The majority of the techniques significantly improved the thermal insulation of concrete composites; nevertheless, each technique has its own set of limits in terms of concrete mechanical strength, cost, and applicability. In comparison to other insulating materials and procedures, Seashell has the unique ability to improve the thermal insulation, acoustic insulation, and physical qualities of ordinary normal strength concrete at a much reduced cost. The safe and effective disposal of seashell is ensured by its incorporation into concrete composites. Because of its porous structure, it can produce low-density cement composites that are more energy efficient and long-lasting. However, such prospective uses of seashell in high-strength concretes and seashell recycling have never been examined before, and more research is needed in this area.

The concept of increasing the thermal and physical properties of cement, mortar, and concrete composites by introducing seashell, either in its natural state or as ash, with or without treatment, has been the subject of extensive research in recent decades.

(Yang, Yi et al. 2005) evaluated different percentages of dry crushed oyster shells (5, 10, 15, and 20%) as fine aggregate substitution in concrete production (less than 5 mm size). They discovered that as the oyster shell substitution rate increased, the concrete's workability, as measured by the slump test, decreased. They also discovered that after 28 days, the compressive strength of concrete was unaffected.

(Panda, Behera et al. 2020) created twelve concrete mixtures. All of the concrete mixes were made by replacing 10%, 20% and 30% of the fine aggregate with crushed seashells and 0, 10% and 20% of the cement with RHA. The M30 grade mix design was used in this experiment. Fresh samples of various concrete mixtures were tested to measure slump and other properties. Hardened samples were tested for compressive, split tensile and flexural strength after 7, 28, and 90 days of curing in water. When compared to crushed seashell-based concrete mixes, the findings of the trials demonstrate that employing RHA-based concrete mixes improves strength. When crushed seashells are replaced with fine aggregate, the strength of seashell-based concrete steadily declines.

Furthermore, it has been discovered when RHA is used as a cement replacement, there was an increase in strength of all concrete mixes. The results show that adding additional seashell aggregate to concrete reduces workability, and that the water absorption of seashell aggregate is larger than that of regular aggregate.

(Nguyen, Boutouil et al. 2017) investigated the durability of pervious concrete with and without crushed seashells using freeze-thaw resistance tests, clogging tests, and leaching tests. Crushed seashells replaced 60% of the natural particles in the control pervious concrete to generate the shell pervious concrete. The shell pervious concrete's freeze-thaw resistance was lower than the control pervious concrete's and was not proportional to mechanical strength. Furthermore, when a blended mixture containing silty clay and sand is utilized as a clogging agent, the drainage capacity of pervious concrete is greatly reduced. The pervious concretes, on the other hand, remain permeable even after blockage ($k > 0.5$ mm/s). Furthermore, when pervious concretes come into touch with demineralized water, they leach quickly. This experiment also revealed that several chemical qualities of broken shells (chloride ion and organic matter content) may have a superior impact on durability as compared to physical and mechanical properties of pervious concrete.

(Bamigboye, Enabulele et al. 2021) explains the various waste seashells used, the growing global aquaculture production, seashell material preparation and treatment, physical properties, chemical composition, and various mechanical (compressive, split tensile, flexural strength, and modulus of elasticity) and durability test methods. The study discovered that the compressive, splitting tensile and flexural strength of concrete decreases as there is an increase in the seashell percentage; the modulus of elasticity is lower than the control specimen; shrinkage increases with increase in seashell percentage and the seashell waste has more water absorption capacity as compared to natural sand.

(Panda, Gouda et al. 2020) created thirteen concrete mixes. The first is traditional concrete, while the second is made by partially replacing fine aggregate with crushed seashell and cement with GGBS. Crushed seashell was added to the ordinary concrete in proportions of 0%, 10%, 20% and 30%, respectively. Then 10% seashell mix concrete was combined with 10%, 20% and 30% GGBS mix concrete, similarly 20% and 30% of seashell mix concrete was mixed with 10%, 20% and 30% of GGBS mix concrete, respectively. A concrete mix of M30 grade was prepared for this experiment. Slump tests for concrete workability were performed on various mixes of new concrete, and it was discovered that increasing the amount of seashell aggregate in concrete affects the workability of the concrete. After 7 days and 28 days of curing under water, tests such as compressive, split-tensile, and flexural strength were performed on hardened concrete samples of various mixes. Experiments show that using seashell in concrete reduces the strength over time, whereas using GGBS increases the strength over time in all types of concrete mixes. The result declares improved compressive, flexural, and split-tensile strength with a 10% partial replacement of fine aggregate with crushed seashell and a 20% partial replacement of cement with GGBS.

(Varhen, Carrillo et al. 2017) substituted Peruvian scallop crushed seashell (CSS) with fine aggregate at various percentages (0, 5, 20, 40, and 60%) with varying w/c ratios of 0.75, 0.55, 0.45, and 0.41 and checked for fresh and hardened properties of concrete after 7, 28, and 90 days. The outcomes show that clean CSS may take the place of fine aggregate. Because of the angular shape of CSS, the amount of cement required to maintain the same workability must be increased. If the w/c ratio increases, replacement should be reduced. CSS replacement of 5% improves the fresh and hardened state properties. Despite the fact that CSS sizes range from 1.19 to 4.75mm, 40% replacement can be done without losing fresh and hardened properties.

(Lertwattanaruk, Makul et al. 2012) explored four varieties of waste seashells in this research, including the short-necked clam, green mussel, oyster, and cockle, in order to develop a cement product for building and plastering. Water demand, setting time, compressive strength, drying shrinkage, and mortars' thermal conductivity were studied. These characteristics were compared to those of a standard mortar and were constructed using a standard Portland cement. The proportion of powdered seashells as a substitute for cement was 5, 10, 15, or 20% by weight.

Ground incorporated seashells resulted in a reduction in water consumption and an extension of the setting durations of mortars, which are in hot regions; there are several advantages to rendering and plastering. Mortars made with ground seashells have adequate strength, less shrinkage after drying, and lower thermal conductivity than normal cement. The findings suggest that ground seashells can be used in place of cement in mortar formulations, which could make rendering and plastering easier.

(Safi, Saidi et al. 2015) determine the feasibility of using or recycling trash from Marin, namely seashells, which is used as a replacement of sand in self-compacting mortars (SCMs). The properties of self-compacting mortars (SCMs) were evaluated in their fresh (flowability and fluidity) and hardened states (porosity/water absorption, bulk density, compressive and flexural strength, and elastic modulus) with and without the addition of crushed seashells (Sh) at various ratios (Sh/S = 0, 10, 20, 50, and 100%) by weight. Crushed seashells (0/5 mm class) can be used as sand in self-compacting mortar without compromising the mortar's basic properties, according to the findings. The flowability of mortars made solely of seashells, on the other hand, was superior and proved adequate for fluid concrete (as a self-compacting concrete). Furthermore, replacing sand with crushed seashells up to 100% resulted in a small reduction in the elastic modulus and compressive strength of the mortars studied. Using an optical microscope, a macro-structural investigation of the interfacial zone (seashells–binder) indicated that the seashell and cement paste adhere well, and that the angular shape of the seashells significantly enhanced the latter's dispersion in the cementitious matrix.

(Martínez-García, González-Fonteboa et al. 2019) explained that millions of tonnes of farmed mussels are produced annually in over 40 nations. This procedure generates a lot of shell waste, which has a big impact on the environment. A low-impact heat treatment procedure is utilized in Galicia to turn mussel shell waste into a by-product that may be used as an aggregate. This research examines cement-coating mortars with a portion of conventional aggregate replaced by mussel shell aggregate. This studies evaluated reference mortars and mortars with varying percentages of mussel shell i.e., 25, 50, and 75% as a replacement of natural sand. The results demonstrate the viability of using mussel shell in cement coatings at a 25% replacement rate for conventional aggregate.

2.5 High strength concrete material properties at elevated temperature

Critically viewing at the literature, it can be seen that HSC at elevated temperature behaves differently from NSC in two ways (Phan and Carino 1998).

- Higher magnitude of strength loss induced by elevated temperature than NSC in a temperature range of 100°C to 400°C.
- Failure due to spalling of concrete with an explosion at rapidly increasing rate of temperature which is again in contrast with NSC.

Different test variables influence the rate of strength loss as temperature rises and the rate of explosive spalling. Combination of load application time and heating scenario (stressed, un-stressed, and unstressed residual) (Phan and Carino 2002), initial moisture content of the specimen before fire testing (Chan, Peng et al. 1999), water-cementitious ratio (w/cm), sand ratio, quantity of silica fume and its ratio (Bastami, Chaboki-Khiabani et al. 2011), heating and cooling rate (Luo, Sun et al. 2000), aggregate type (light weighted or normal weighted), and polypropylene addition are some of them. When study the fire behavior of concrete, whether HSC or NSC, there is a shortage of testing criteria. Different authors use different testing parameters, but for HSC, the rate of heating concrete specimens is kept to (2°C-5°C)/min and a cylinder size of 200mm height x 100mm diameter is used (Hoff, Bilodeau et al. 2000, Cheng, Kodur et al. 2004, Poon, Shui et al. 2004), but other sizes are also used by some researchers, such as 300 mm x 150 mm diameter by (Husem 2006).

2.6 High temperature testing methods based on heating and loading regimes

For heat treatment and testing samples, there are three main testing methods available: stressed, unstressed, and residual. In the pre-heating stage, the specimen is loaded to 40% of its ultimate strength in a stressed condition. The sample is then heat treated to the desired temperature in a predetermined ramp time, and the temperature is then maintained at that temperature for a reasonable period of time to achieve thermal steady state. The load is then increased until the sample fails. Figure 2.2(a) depicts it schematically. This situation simulates real-life fire action. It's a complicated system, thus specific laboratories have been set up to research the fire qualities of members in this situation.

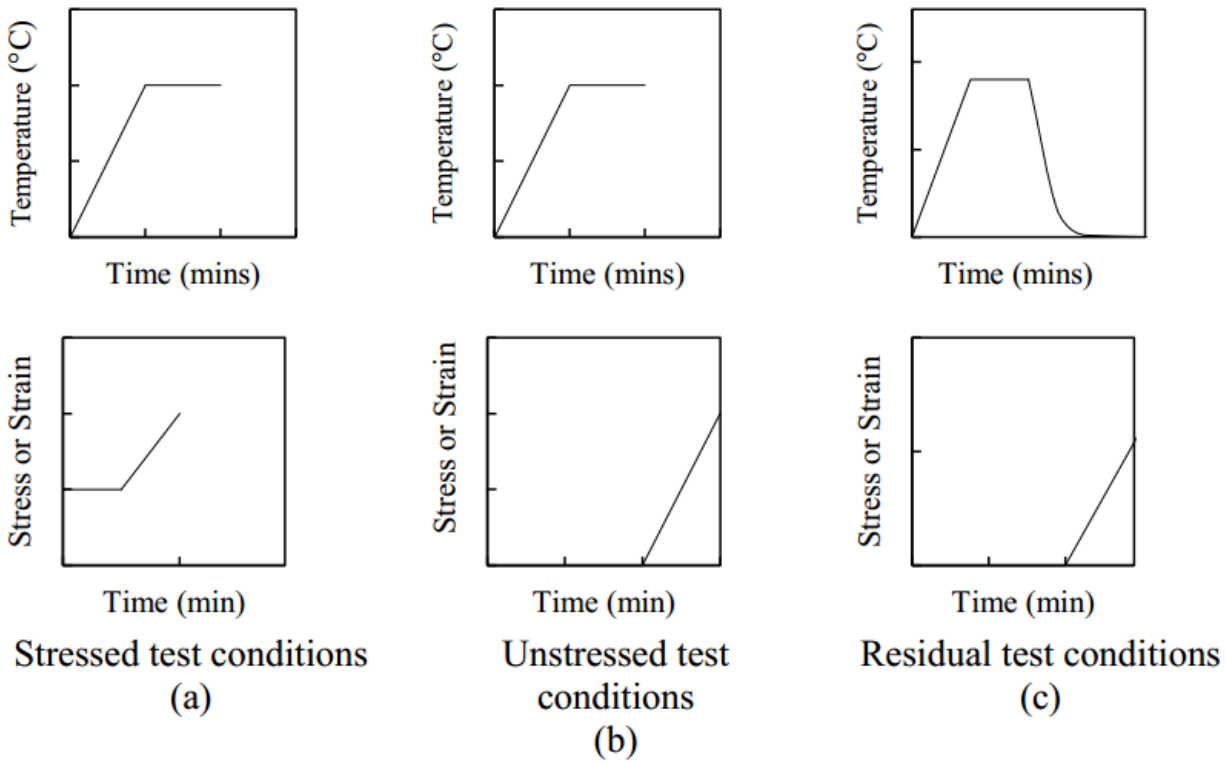

Figure 2.2 Loading and heating conditions for test methods a) stressed b) unstressed c) residual (Kalifa, Menneteau et al. 2000)

In an unstressed condition, the sample is not pre-loaded. The sample is firstly heated to a target temperature and then held that temperature constant for such a period of time to reach thermal steady state. After that, the sample is evaluated without losing any heat by insulating it with a thermal jacket. The results obtained differ from those obtained under stressful settings, but they provide a reasonably accurate picture of how the structure will function under actual fire conditions. Figure 2.2(b) is a schematic representation.

In a residual situation, the specimen is heated under steady-state circumstances and subsequently cooled to ambient temperature. The sample is then loaded till it fails. Figure 2.2(c) depicts the loading and heating procedures. This condition is the least accurate, but it is easy and simple to implement, and as a result, most high-temperature research is based on this method.

2.7 Rapid cooling/quenching method

After specimens have been exposed to elevated temperatures, the method used to cool them to room temperature has a significant impact on strength degradation. Previous study has found that rapid/fast cooling/quenching causes more compressive strength degradation than normal cooling by air, commonly known as the residual test method, due to the rapid/fast cooling technique's larger crack formation (Nadeem, Memon et al. 2014). After being exposed to high temperatures, samples were sprayed with water to cool quickly (Nassif, Rigden et al. 1999, Awal, Shehu et al. 2015). The specimen was rotated in front of the tap nozzle for 5 minutes to achieve uniform spraying (Nassif, Rigden et al. 1999, Peng, Bian et al. 2008). After that, the specimen was allowed to cool entirely to room temperature.

2.8 Previous investigations on mechanical performance of concrete exposed to elevated temperatures

This section provides a summary of published data on the variation of mechanical properties of concrete at various elevated temperatures, such as compressive and cracking tensile strength, elastic modulus, stress-strain response, and mass loss. Heating rate, test methods (stressed, unstressed, or unstressed residual), size of the test specimen, moisture content during heating, type of coarse aggregates, strength (NSC or HSC), cement content, type of SRM (fly ash, silica fume, etc.), type of cement, and so on all affect the variation of these aspects of concrete as a function of temperature. Because all of the information is rarely found in a single study, it is impossible to consider each unique aspect from each study for comparison reasons. A general overview of the research on concrete's fire behavior is offered.

2.8.1 Compressive strength

Compressive strength is the most basic and crucial mechanical property of concrete, as it is the primary input parameter in the structural design of RCC parts. Concrete is structurally active in compression in the majority of grey constructions. The difference in concrete compression strength with regard to temperature must be known as an input parameter for the creation of prediction models of the structural performance of RCC elements subjected to elevated temperatures.

(Ali, O'Connor et al. 2001) A review of a number of studies on the variation of concrete strength under compression at elevated temperatures is presented, with the conclusion that the disparity in compressive resistance of concrete with respect to temperatures is influenced by a number of factors, including strength at room temperature (NSC or HSC), nature of loading and heating regimes (stressed, unstressed, or unstressed residual), heating rate, type of coarse aggregate (normal weight siliceous and calcareous, or lightweight), moisture content and the porosity of concrete which is highly affected by the presence of SRM (SF, FA and GGBFS etc.).

Because the microstructure of HSC is denser and impermeable, the steam pressures created by high temperatures are not escaped, the degradation of compressive strength as a function of temperature is more evident in HSC than in NSC. In terms of relative compressive strength loss, HSC loses up to 40% of its room temperature strength between the temperatures of 100°C and 400°C, whereas NSC loses 10 to 20% of its room temperature strength in the same temperature range (Phan and Carino 2001).

SRMs have long been recognized as necessary components in the production of high-performance concrete (HPC). SRMs not only make concrete production more cost-effective, but their proper application can also result in concrete that is superior to ordinary concrete. The presence of a certain SRM in concrete can affect its fire behavior in either a negative or positive way. The presence of FA and GGBFS has been shown to improve concrete's reaction to fire, whilst the presence of SF and MK has been shown to have a negative impact on concrete's response to fire (Poon, Azhar et al. 2001, Poon, Azhar et al. 2003).

(Ergün, Kürklü et al. 2013) investigated the impact of two different cement concentrations, 250 and 350 kg/m3, on the behavior of concrete at high temperatures. He employed limestone aggregates, ordinary Portland cement (OPC), a 0.50 w/c ratio, and a 2°C/min heating rate. Compressive strength tests were performed on cubes with dimensions of 150X150X150 mm. Mixtures with cement concentrations of 250 and 350 kg/m3 had room temperature compressive strengths of 28.16 and 48.99 MPa, respectively. He looked at how compressive strength changed under unstressed residual conditions after test specimens were exposed to five different target temperatures: 100, 200, 400, 600, and 800 degrees Celsius. Each temperature was kept constant for 45 minutes to ensure that each specimen reached thermal equilibrium. Figure 2.3 depicts the decrease in compressive strength as the target temperature rises.

They came to the conclusion that cement dosage had little effect on the behavior of concrete at high temperatures. (Netinger, Kesegic et al. 2011) researched the effects of two distinct types of aggregates on the performance of concrete exposed to high temperatures: dolomite (calcareous) and diabase (siliceous). He used OPC with a 450 kg/m3 fixed cement content and a 0.50 w/c ratio.

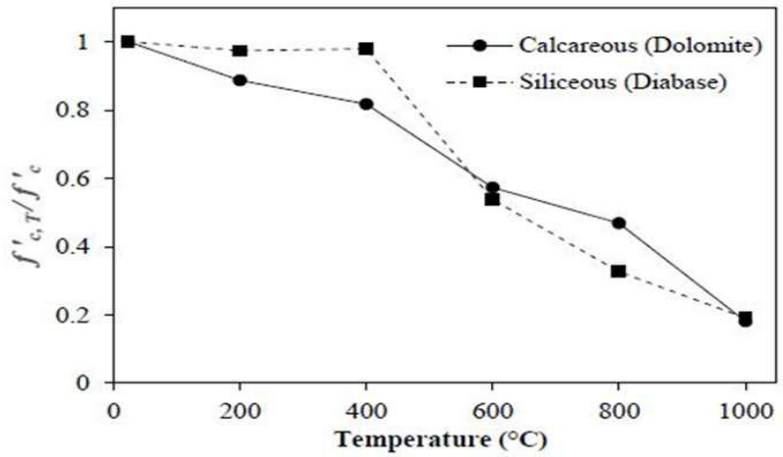

Figure 2.3 Normalized compression strength trends at various temperatures (Ergün, Kürklü et al. 2013)

Concretes containing calcareous (dolomite) and siliceous (diabase) aggregates had compressive strengths of 45.9 and 38.3 MPa at ambient temperature, respectively. Compressive strength testing was performed on 4 x 4 x 8 cm prisms. Concrete specimens were heated in an electric furnace for 1.5 hours at five different target temperatures: 200, 400, 600, 800, and 1000 degrees Celsius. After being exposed to high temperatures, the specimens were cooled to room temperature, and then loads were applied until the specimens failed. He found that the deterioration of compressive strength for concrete containing siliceous (diabase) coarse aggregates is less as the temperature rises from 200°C to 400°C, whereas the degradation of compressive strength for concrete containing calcareous (dolomite) coarse aggregates is less as the temperature rises beyond 400°C. The findings of this investigation are shown in Figure 2.4.

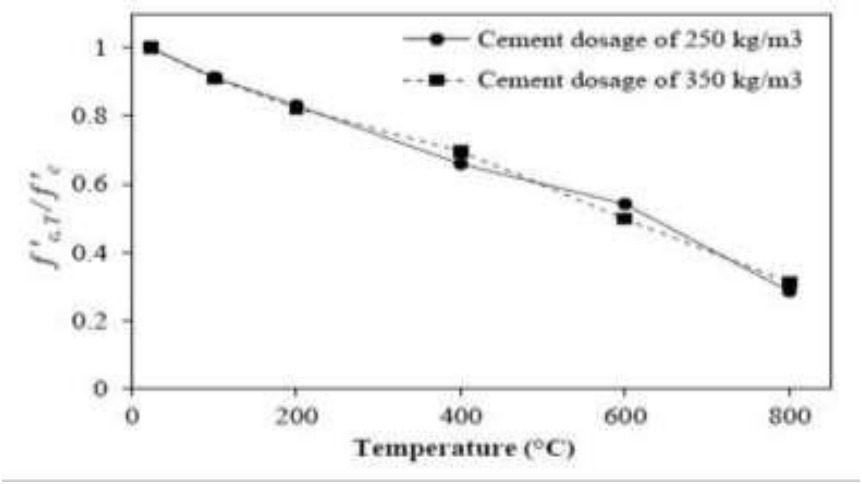

Figure 2.4 Variation of normalized compressive strength as a function of temperature (Netinger, Kesegic et al. 2011)

2.8.2 Stress-strain response

Concrete stress-strain response is critical because it is a key input parameter in mathematical models that anticipate a concrete structural member's response. To use a numerical method such as finite element analysis to simulate the response of a concrete structural member exposed to fire, a constitutive model of concrete must be available that can capture the strains at various stress levels and temperatures. Concrete gets increasingly porous as the temperature rises, and this increase in porosity leads concrete to become more ductile in compression. As a result, the slope of stress-stain curves reduces as exposure temperatures rise (Kodur 2014). With rising temperatures, the strains corresponding to peak stresses and ultimate stresses tend to rise as well (Knaack, Kurama et al. 2011).

(Cheng, Kodur et al. 2004) used selection residual testing to study the stress-strain response of HSC at various high temperatures. A 2°C/min heating rate was chosen. The compressive strength at ambient temperature was 71.4 MPa. The test specimens were cylinders measuring 100 x 200 mm. The stress-strain response was measured using a strain-controlled loading technique. Figure 2.13 shows the measured stress-strain response at progressively high temperatures. They discovered that when exposure temperatures rise, the slope of stress-strain plots decreases. They also discovered that peak strains at higher temperatures can be up to four times higher than peak strains at lower temperatures.

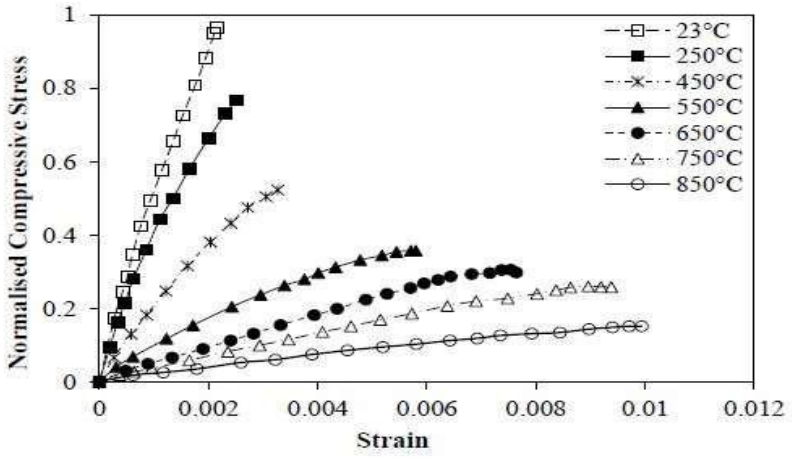

Figure 2.5 Stress-strain response at elevated temperatures (Cheng, Kodur et al. 2004)

2.8.3 Elastic modulus

The modulus of elasticity of concrete is an important material attribute since it is used to calculate the deflections of a concrete structural part. It is also a required input parameter while performing RCC frame elastic frame analysis. The w/c ratio, the age of the concrete, the techniques of conditioning after casting, the kind of aggregates, and the number of aggregates all influence the elastic modulus of concrete (Kodur 2014). At high temperatures, the elastic modulus of concrete, like other material properties, changes.

(Xiao, Li et al. 2016) looked at the difference in secant modulus as a function of temperature. They used a 2.5°C/min heating rate and a 2.5-hour hold time. The water to cement ratio was 0.24, and the powder content was 580 kg/m3. GGBFS was used to replace 20% of the cement mass, and SF was used to replace 10% of the cement mass. HSC's compressive strength and elastic modulus at room temperature were 68.36 MPa and 38.22 GPa, respectively. Prisms measuring 100 x 100 x 300 mm were used. Figure 2.6 depicts the reported variation in elastic modulus as temperature rises. In the temperature range of 23 to 200°C, they discovered a significant drop in elastic modulus. From 200 to 400°C, the rate of degradation became more consistent, but from 400 to 600°C, the most pronounced rate of degradation was observed. A decrease in the rate of elastic modulus reduction was observed at temperatures above 600°C. Calcination of limestone aggregates was blamed for the reduced rate of drop in elastic modulus beyond 600°C.

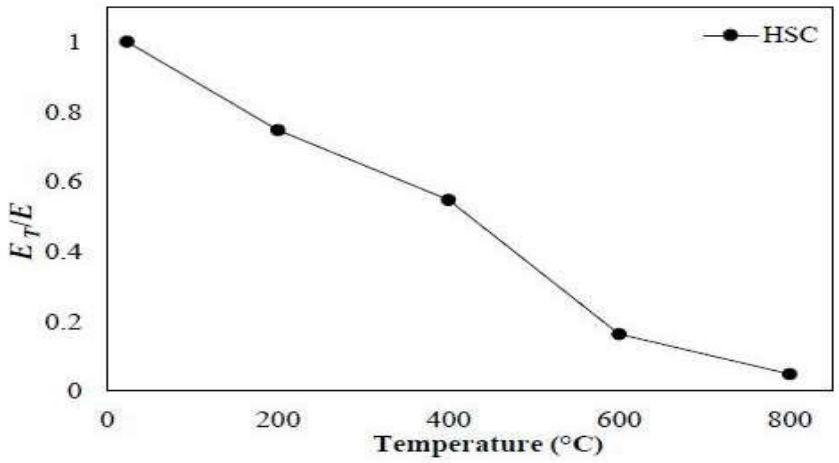

Figure 2.6 Normalized secant modulus trends as a function of temperature (Xiao, Li et al. 2016)

2.8.4 Mass loss

The mass of concrete decreases as the temperature rises. Thermo-gravimetric analysis is a technique used by material analysts to assess the composition of a substance by measuring the mass loss of a material as temperature rises. Thermo-gravimetric analysis, in which the sample is gradually heated at a rate of 10°C/min and the resulting mass loss is observed as the temperature rises. A graph of % mass losses vs. temperature has been created. This is compared to similar graphs of materials with known compositions, yielding useful information on the chemistry of the material in question. This approach is typically used on pastes rather than concretes in concrete technology since concrete also contains aggregates with varying mineral compositions, which would make accurate assessment of the true chemistry of a concrete's pastes difficult. The same technique is used to determine the extent of pozzolanic activity of various pozzolanas by measuring the mass loss of pastes at temperatures equivalent to calcium hydroxide dissociation (400 to 600°C) (Rizwan 2006). Still, different scholars offer mass losses of concrete at high temperatures, possibly in an attempt to get a broader picture of the changes in concrete at high temperatures. Moisture migration, heat degradation of the concrete's elements, and spalling are the three main causes of concrete mass loss as temperatures rise (Kodur 2014).

In HSC, concrete that has been exposed to greater temperatures has a tendency to spall. Large pieces of concrete are detached from the surface of the concrete specimen during explosive spalling, which can account for a significant amount of mass loss. Because mass loss is used to analyze the change in the mass of cylindrical specimens caused by temperature increases, mass loss for those specimens that have spalled is ignored because it will not offer any information on mass loss owing to disintegration.

Moisture migration accounts for the majority of concrete mass loss at high temperatures. C-S-H gel and calcium hydroxide are the key constituents in hardened cement pastes. As the temperature of concrete rises, the free moisture (which is not chemically bound) evaporates out of the concrete until 150°C, the second main mass loss occurs between 400-500°C as CH (calcium hydroxide) is decomposed into CaO (calcium oxide) and water vapors, and beyond 600°C, the third main mass loss occurs as calcium carbonate (if coarse aggregate) decomposes into CaO (calcium oxide) and water vapors. There are peaks in mass losses at these three temperature stages, but there is also a somewhat continuous mass loss due to C-S-H dehydration, which begins at 400°C and lasts until around 900°C (Akca and Zihnioğlu 2013). Concrete loses strength fast beyond 400°C because chemically bonded water in C-S-H begins to free at 400°C. Initial mass loss up to 600 °C is primarily due to moisture migration, either free moisture or chemically bound moisture, hence the primary elements that contribute to the amount of mass loss in this temperature range are moisture content and concrete permeability. Because NSC contains more moisture due to a larger w/c ratio and is also more permeable than HSC, mass loss in NSC is greater up to 600°C (Phan and Phan 1996). Figure 2.7 shows mass losses as a function of temperature for two concrete mixes: NSC and HSC, as published by (Khaliq 2012). These concrete mixes were made with calcareous aggregates that were similar in nature. It can be seen that the extent of mass loss in NSC is more than in HSC up to 600 °C. Because of the breakdown of calcareous aggregates present in both HSC and NSC, both mixtures lose mass at 600°C.

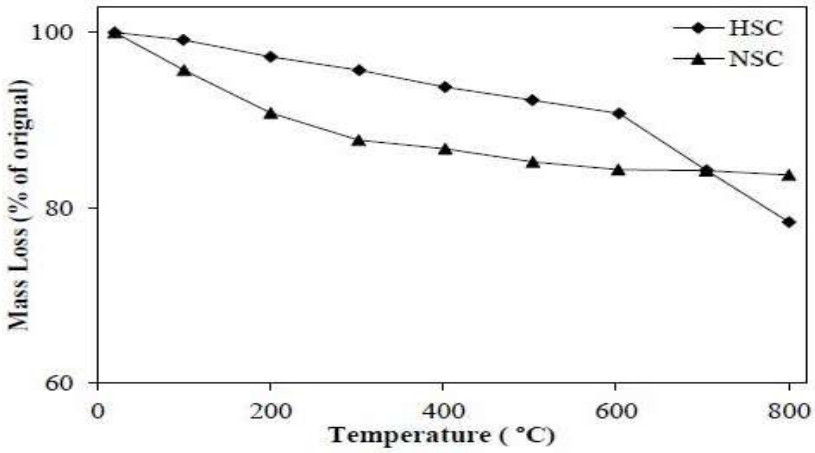

Figure 2.7 Mass loss as a function of temperatures (Khaliq 2012)

The type of aggregates used in concrete has a direct impact on the mass retention of concrete at temperatures above 600°C. Beyond 600°C, concretes containing calcareous aggregates show significant mass loss, which can be attributable to the breakdown of calcium carbonate in the aggregates. In contrast, mass loss beyond 600 °C for concretes containing siliceous aggregates is negligible. In Figure 2.8, (Kodur 2014) collated data on mass loss as a function of temperature published by several studies for concretes including either calcareous or siliceous particles. It can be seen that mass loss for calcareous concretes is rapid beyond 600°C, whereas mass loss for siliceous concretes is negligible beyond 600°C.

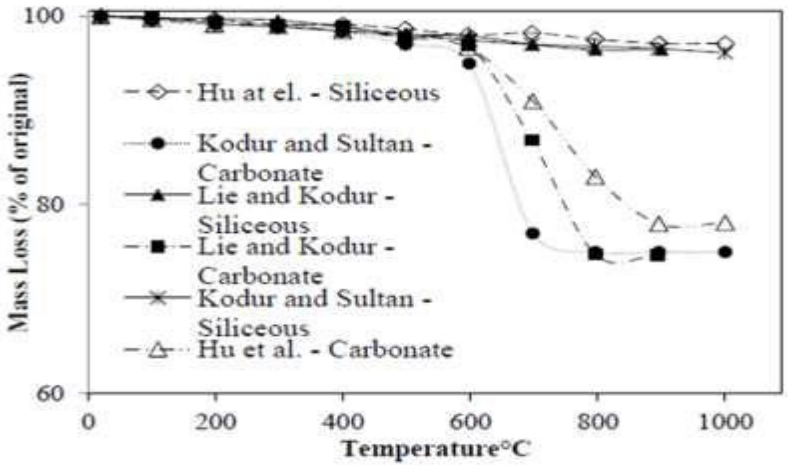

Figure 2.8 Mass loss at various elevated temperatures (Kodur 2014)

2.8.5 Microstructural changes causing drop in mechanical strength

The major binding agent in concrete is calcium silicate gel, which is made up of cement and water. Concrete's mechanical strength deteriorates when its binding qualities deteriorate. When the concrete specimen is heated to a higher temperature, the moisture in the calcium silicate gel evaporates, disrupting the van der walls forces between the aggregate and the gel, weakening the link between them. As a result, at temperatures exceeding 100°C, the mechanical strength of concrete is reduced (Lankard, Birkimer et al. 1971). At 200°C, there is a minor strength recovery, which is thought to be related to the general stiffness of calcium silicate gel or the re-establishment of the binding between aggregate and gel as a result of the evaporation of adsorbed moisture (Castillo and Durrani 1990). The density of the microstructure affects the evaporation of adsorbed water. Rehydration of calcium silicate gel owing to temperature increase is also contributed to strength recovery between 100°C and 300°C (Lie and Kodur 1996). The temperature that corresponds to the peak point in the strength recovery phase is not constant, and it varies depending on the moisture content and density of the concrete microstructure.

The dissolution of calcium silicate gel occurs at temperatures above 300°C. Furthermore, at this temperature, the aggregates expand, and the calcium silicate gel shrinks due to moisture evaporation (Georgali and Tsakiridis 2005, Janotka and Nürnbergerová 2005). On a wider scale, this simultaneous expansion and shrinkage creates a loss of link between the aggregate and the gel. As a result, substantial strength decrements have been reported in both high and low strength concrete (Menzel 1943). Calcination of limestone aggregates occurs above 600°C and above in the limestone-based coarse aggregates employed in this study (Lie and Kodur 1996). As a result of the calcination of coarse aggregates, a sudden loss in mechanical strength is observed.

2.9 Previous investigation on mortars under elevated temperature

In this section summary of different researches on mortar under elevated temperature is going to be discussed for comparison purpose.

(Sikora, Cendrowski et al. 2018) studied the effects of Fe_3O_4 and Fe_3O_4/SiO_2 nanoparticle admixtures on the behavior of cement mortars exposed to high temperatures. To generate a core-shell nanostructure (Fe_3O_4/SiO_2), pristine magnetite (Fe_3O_4) nanoparticles were covered with a solid silica shell (through the Stöber process). The cement mortars had an optimal Fe_3O_4/SiO_2 admixture ratio of 3% wt Fe_3O_4 and 5% wt Fe_3O_4/SiO_2 admixtures. Temperatures of 200, 300, 450, 600, and 800 °C were applied to the specimens. The compressive strength, flexural strength and mass loss of the specimens were measured after cooling. The findings showed that magnetite-silica (Fe_3O4/SiO_2) nanostructures are far more advantageous than clean Fe_3O_4 nanoparticles for enhancing the heat resistance of cement mortars. The silica (SiO_2) shell in the nanoparticles increases residual compressive strength and minimizes fracture extension in cement mortars when exposed to high temperatures. Optical and scanning electron microscopic techniques were used to support the findings of this study.

(Horszczaruk, Sikora et al. 2017) investigated the effect of nanosilica (NS) on the behavior of cement mortars comprising quartz aggregate and two types of heavyweight aggregates (barite and magnetite) when subjected to high temperatures. Nanosilica (by weight of cement) has been added to the cement mortars at concentrations of 1, 2, 3, 4, and 5%. The samples were heated to 200, 400, 600, and 800°C, respectively. For the cooled specimens' mass loss, compressive, and flexural strengths were measured. Structure flaws have also been determined using scanning electron microscopy (SEM) and optical microscopy. Results reveal that a high nanosilica concentration in a cement mortar including magnetite and quartz aggregate increases heat resistance and avoids fracture extension (mostly in between 200 and 400 °C). However, due to the aggregate's low heat resistance, cement mortars having barite aggregate tend to crack and spall, according to the study.

(Abeer, Hasan et al. 2020) has major goal is to see how waste material (lightweight concrete blocks) may be used to partially replace fine aggregate. At temperatures of 24, 200, 400, and 600 °C, 168 mortar specimens (84 cubes and 84 prisms) were made using seven mix designs with replacement ratios of 10 and 20% waste material as a replacement of natural sand. Mixed waste lightweight concrete blocks with waste clay bricks or mixed waste lightweight concrete blocks with waste glass were then tested with fiber and without fiber in a single batch (1 percent polypropylene fiber by volume). Mortar specimens were tested for fresh density, flow rate, weight loss, water absorption, compressive and flexural strength. At the age of 28 days, the toughened tests were implemented. The results showed that when using recycled materials, notably scrap lightweight concrete blocks, fresh density decreased by 20%. When normal sand was replaced with waste materials, compressive strength improved, and this improvement was visible at high temperatures. At various temperatures, the specimens that used waste lightweight concrete blocks with waste glass aggregate showed a significant decrease in water absorption when compared to the control mix.

2.10 Surface finishing of specimen

In contrast to concrete cubes, cylinders cast in concrete will always have at least one surface that is quite rough and has many undulations. When the surface is placed in a compression testing machine in its natural state, that is, without adequate surfacing, stress concentration occurs in particular locations, resulting in high compressive strength inaccuracies. Surface planeness tolerance is established in (Astm 2015) to avoid these types of mistakes in compressive strength.

To deal with these inconsistencies, a variety of strategies are employed. According to (Astm 2015), the most typical method is to cap the cylinder with gypsum or sulphur (in the case of HSC). According to (C1231/C1231M-12), the unbonded caps are sometimes employed to save time when capping the cylinders with gypsum or sulphur. Both of the aforementioned procedures are highly useful and precise. However they can be employed after high-temperature testing. The end surfaces of concrete cylinders that do not fulfill the planeness criteria of (Astm 2015) are capped and flattened to meet the planeness criterion in that manner. The compressive strength test, which was conducted with the surface end conditions varied, revealed that the ground end results were consistent with the sulfur-capped cylinder ends.

Table 2.3, which was generated from the experimental program of (Carino 1994), shows such a comparison. Table 2.3 shows that the compressive strength of the surface ground specimen and the sulphur capped specimen are almost identical at almost all strength levels. As a result, the sulphur capped technique is applied in this research.

Table 2.3 Comparison between compressive strength of sulphur capped cylinder and surface ground cylinders

Design/Nominal strength (MPa)	**Ground ends cylinder compressive strength (MPa)**	**Sulphur capped ends cylinder compressive strength (MPa)**	**Loading Rate(Mpa/sec)**	**Specimen Diameter (mm)**
90	91.28	86.29	0.34	150
	88.12	86.14	0.14	150
65	69.16	68.81	0.34	150
	68.71	67.38	0.14	150
45	45.84	44.75	0.34	150
	44.77	43.64	0.14	150

CHAPTER 3

EXPERIMNTAL PROGRAM

3.1 General

The methodology used to achieve research aims has been addressed in this chapter. The procedures for preparing the specimen as well as the testing procedures used to acquire the results are described in full.

Mechanical, material, and physical properties of both types of concrete mixes are necessary for investigating and assessing the performance and responsiveness of both HSC and SS-HSC at elevated temperatures. Compressive strength, compressive stress-strain response, thermal stresses and mass loss are all material properties of concern in concrete. The material properties of HSC are well-documented in the literature, but there is no information on the mechanical properties of SS-HSC at higher temperatures. As a result, determining the mechanical and material properties of SS-HSC at higher temperatures is crucial in order to determine the strength loss as temperature rises. High-temperature mechanical property tests on concrete specimens were carried out to sort out the effect of higher temperatures on the material properties of SS-HSC, including compressive strength, stress-strain behavior, secant modulus, compressive toughness, thermal stresses and mass loss. Then, all of the mechanical and material properties results are graphed, and this data is utilized to develop numerical models for various material properties as a function of temperature in the range of 23°C to 800°C. This chapter discusses the detailed experimental work, testing rigs, processes, and standards needed to perform various mechanical and thermal property tests.

3.2 Material

3.2.1 Seashell

A seashell or sea shell, also known simply as a shell, is a hard, protective outer coating produced by a sea animal. The shell of the animal is a part of its body. Beachcombers frequently find empty seashells washed up on the shore. This study makes use of a natural seashell found on the coast of the Arabian Sea in Karachi, Pakistan.

Figure 3.1 depicts the seashell utilized in the investigation. Seashell was collected from Karachi's seashores and was grinded from PCSIR Lab, Peshawar and then used in untreated form in the concrete mix design. Size of seashell used for concrete specimens were 1.18 to 0.15mm and under 0.15mm size were used for mortars (coating of concrete).

Figure 3.1 Seashell sample

3.2.1.1 Physical properties of seashell

Sieve analysis was carried out as per ASTM C33 to determine particles size of the seashell sample (equal to sand).

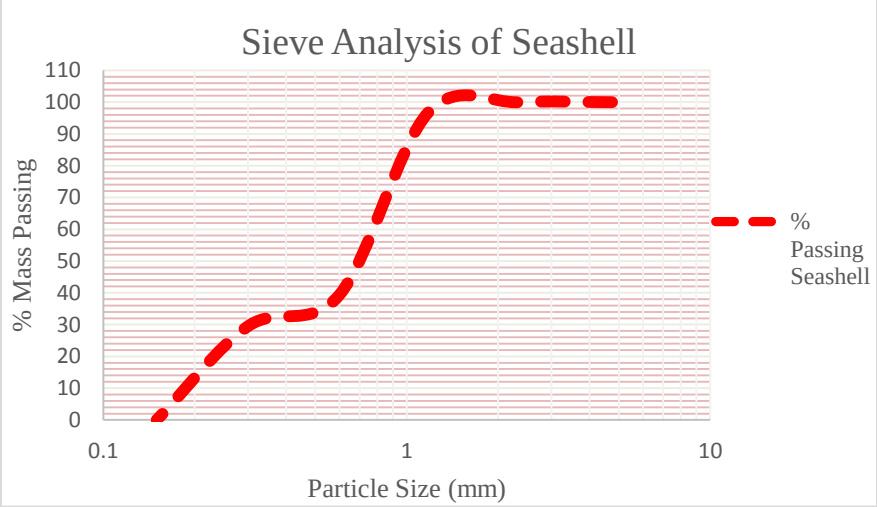

Figure 3.2 Sieve analysis of seashell sample

3.2.2 Cement

Type-I Ordinary Portland Cement (OPC) of Askari Cement was chosen as a binder for HSC, SS-HSC and SP-HSC formulations, according to ASTM C150/C150M-15 (ASTM 2017).

3.2.3 Fine aggregates

The study employed locally accessible Lawrencpur area sand with a fineness modulus (F.M) of 2.3. The sand was clean and free of organic contaminants, and it was employed in a saturated surface dry state. Table 3.2 lists some of its most important physical features as determined by laboratory studies.

Table 3.1 Summarizes the results of sieve analysis on fine aggregate (sand)

Sieve No.	Rt wt	Rt %	Cum. Retained %	Passing %	ASTM C33-03
4	0	0	0	100	95 -100
8	0	0	0	100	80-100
16	25	3	3	97	50-85
30	456	58	61	39	25-60
50	78	9	70	30	30—10
100	234	30	100	0	02—10
200	**0**	0	100	0	
Pan	0	0	100	0	

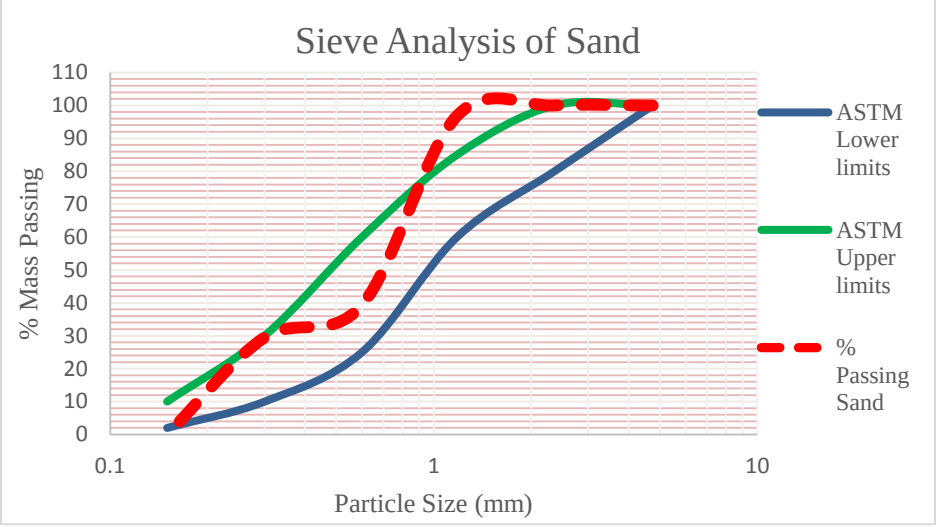

Figure 3.3 Sieve analysis of sand

3.2.4 Coarse aggregates

For the current investigation, Khairabad crush delivered normal weight aggregates consisting of crushed angular stone. In a saturated surface dry condition, coarse aggregates with a maximum size of 12.5mm according to ASTM C33 (C33 2003) and a specific gravity of 2.68 were used (SSD). Some of its physical characteristics, as determined by lab tests, are listed in Table 3.2.

Table 3.2 Physical properties of fine and coarse aggregate

Sr. No	Properties	Results
1	Max Coarse Aggregates Size	12.5mm
2	Fineness Modulus (sand)	2.3
3	Specific Gravity of Fine Aggregates (SSD)	2.65
4	Impact Value of Coarse Aggregates (%)	6.38%
5	Specific Gravity of Coarse Aggregates (SSD)	2.68
6	Crushing Value of Coarse Aggreagte (%)	17%

Figure 3.4 Test setups for physical properties of aggregates

3.2.5 Mineral and chemical admixtures

Silica Fume was employed as an admixture in this investigation. Silica fume has a high density and a tiny average particle size, resulting in a better microstructure in the concrete. The silica fume utilized had a bulk density of 660 kg/m3. Sika Chemical (PVT) LTD, a chemical supplier that also manufactures silica fume, obtained it.

To prepare a workable concrete mix at a very low water-cement ratio, superplasticizer was used. The commercial name of superplasticizer is Viscocrete-3110.

3.3 Experimental work

A complete analysis was carried out to analyze the mechanical and physical properties of HSC including seashell with a comparison of its high-temperature behavior with SS-HSC and SP-HSC in order to obtain data on the performance of SS-HSC and SP-HSC at elevated temperatures. Also the HSC, confined with mortar having seashell replaces sand in the mixture.

3.3.1 Mix proportion

The control formulation used a concrete mix ratio of 1:1.35:2.80 with a water to cement ratio of 0.35. Casting was undertaken in two steps, first step comprises of four high strength concrete formulation i.e. HSC, 10SS-HSC, 20SS-HSC and 30SS-HSC. Second step comprises of three high strength concrete plastering formulations i.e. 20SP-HSC, 40SP-HSC and 60SP-HSC. Detailed mix design for the analyzed formulations is presented in Table 3.3 and 3.4. Four types High strength concretes (HSC) mixes were casted containing 0, 10, 20 and 30% seashell replacement as total dry volume of sand. After 24 hours the casted cylindrical samples were then demoulded. Curing of all the specimens was carried out in the water curing tank at ambient condition of 95% humidity and 23˚C temperature for 28 days. The specimens were then analyzed for physical, thermal and mechanical response in detail. Other high strength concretes mixes for plastering were casted and were coated (plaster) with seashell (as a replacement of sand in mortar) on 28 days strength containing 20, 40 and 60%, respectively. 28 days curing of all the specimens took place. After curing, the specimens were then analyzed for physical, thermal and mechanical response in detail.

Table 3.3 Mix design of various concrete formulations

Mix Id	Cement	Silica Fume	Sand	Coarse Aggregate	Seashell	Water	Superplasticizer
HSC	612	61.2	694	1457	0	236	6.73
10SS-HSC	612	61.2	625	1457	67	236	6.73
20SS-HSC	612	61.2	556	1457	134	236	6.73
30SS-HSC	612	61.2	486	1457	201	236	6.73

Table 3.4 Mix design of various formulations in Kg/m^3

Mix Id	Cement		Silica Fume	Sand		Coarse Aggregate	Seashell	Water	Superplasticizer
	In concrete	In mortar	In concrete	In concrete	In mortar	In concrete	In mortar	In concrete	In concrete
20SP-HSC	612	630	61.2	694	1696	1457	410	236	6.73
40SP-HSC	612	630	61.2	694	1272	1457	819	236	6.73
60SP-HSC	612	630	61.2	694	848	1457	1229	236	6.73

3.3.2 Mixing regime of concrete

The mixing of the concrete ingredients was done with a horizontal concrete mixer as shown in figure 3.5. The mixing of different concrete elements was done according to the specifications provided by (ASTM C192 / C192M 2016) (Standard 2016). The following is a summary of the mixing technique. The mixing water was separated into four parts at first, and then superplasticizer was added to one of the quarters. To begin, coarse aggregates were added to the mixer, along with about a quarter cup of mixing water, and the mixture was allowed to mix for about 2-3 minutes. Second, after adding fine aggregates, the mixture was mixed for another 2 minutes. Third, the binder (cement plus silica fume) was added, along with about two-thirds of the mixing water, and thoroughly mixed. Finally, the leftover superplasticizer was mixed with a quarter of water and the entire mixture was allowed to mix until it reached a homogeneous consistency. The concrete mixer machine was then turned off and allowed to rest for three to four minutes. After the rest, the mixing was continued, with a final mixing time of 2 minutes.

Figure 3.5 Concrete mixer

3.3.3 Specimen preparation and curing details

All of the test specimens were cylinders measuring 4 inches by 8 inches (100mm by 200mm). After correct mixing, three layers of concrete mix were put into the steel moulds, and each layer was rodded according to (ASTM C192 / C192M 2016) (Standard 2016) standards. After 24 hours, the specimens were demoulded and maintained in a water tank to cure at room temperature (23 to 32°C). The cylindrical specimens were removed from the curing tank and placed in a dry area at room temperature after 28 days of moist curing. The plaster samples were plastered after 28 days of concrete casting and cured them for further 28 days. Figures 3.6 show freshly poured concrete specimens in moulds and concrete specimens in the hardened stage, respectively.

Figure 3.6 Preparation of specimens and curing

3.3.4 Capping ends of concrete's cylinders

Concrete's cylindrical specimen has one smooth end which is formed on the base plate of the mold and other rough end. Non formed (rough) ends of all the specimens intended to be used for compressive testing were capped with the help of sulphur capping to bring them well within the permissible tolerances of (ASTM C39 / C39M 2016) (Concrete and Aggregates 2014) on perpendicularity and planeness. Figure 3.7 shows the sulphur capping used for the purpose of smooth end of a specimen.

Figure 3.7 Capping of specimens

3.3.5 Instrumentation

For each mix regime, a similar method of embedding the thermocouples (TC) in concrete cylinders was used to estimate the duration for which a given temperature must be maintained so that the core of the concrete specimen may achieve that particular temperature (Hold time). Each mix has one test cylinder with two thermocouples (TC), one inserted at the surface and the other in the core. Surface TC was implanted by excavating a tiny trench and filling it with thick paste. Drilling a narrow hole from the center of the circular end up to the mid-height of the cylinder and filling it with rich paste was used to implant the core TC. The TC employed in this investigation was K-type, capable of sensing a maximum temperature of 940°C. Heating characteristics of concrete mix are plots that depict the temperature variations of different regions of a concrete specimen over time (Phan and Carino 2001). The instrumentation process and a schematic diagram to demonstrate the heating characteristics determination procedure are shown in Figure 3.8.

Figure 3.8 Instrumentation process and a schematic diagram to demonstrate the heating characteristics

3.4 Material property test

Mechanical characteristics tests, such as compression, elastic modulus, stress-strain response, and compressive toughness tests were performed on all eight mentioned mixes following exposure to the required temperature at a desired heating rate. Aside from mechanical tests, each specimen's mass loss was calculated in residual conditions. This part goes through the specifics of the testing procedure and technique, as well as the testing equipment, testing variables, and specimen fabrication. Table 3.5 lists all of the specimens that were tested at the desired temperature.

Table 3.5 Details of specimens prepared to be tested at desired temperature

Mix Type	Exposure Temperature (°C)	Compressive Strength	Remarks
	Cylinder specimen size 100×200 mm with and without plaster and heating rate of 5°C/minute were used.		
HSC 10SS-HSC 20SS-HSC 30SS-HSC	23 200 400 600 800	2 2 2 2 2	Residual Test Conditions
20SP-HSC 40SP-HSC 60SP-HSC	23 200 400 600 800	2 2 2 2 2	Residual Test Conditions

3.4.1 Test specimens

A total of 70 100mm x 200mm specimens were made for each blend (Figure 3.9), in which 40 are without plaster and 30 are with plaster (having 12.5mm thickness). The fire response of concrete specimens of conventional size used for compressive strength tests, i.e. 300mm x 150mm, is poorly documented in the literature. As a result, a smaller cylindrical specimen measuring 100mm x 200mm was chosen, allowing the results to be easily compared to earlier research.

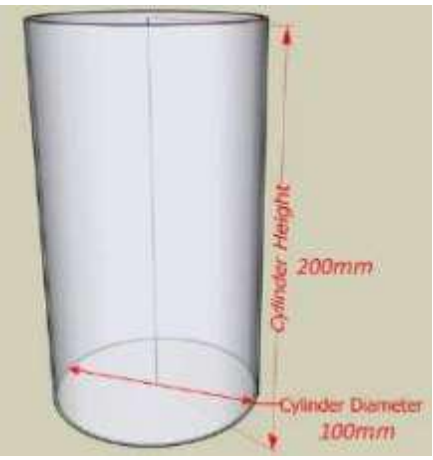

Figure 3.9 Cylinder size and dimensions

3.4.2 Fire loading characteristics

The types of fire loading used have a big impact on the results of specimens. The results are reliant on two fundamental fire loading factors. These are the heating rate and the temperature that you want to achieve. These two parameters were chosen based on previously tested concrete specimens at extreme temperatures due to a lack of high temperature testing standards.

3.4.3 Target temperature

In the high temperature testing of concrete, the most frequently used temperatures on which the mechanical and thermal properties tests are carried out are 23°C (room temperature), along with 200°C, 400°C, 600°C and 800°C.

3.4.3.1 Target temperature for residual test conditions

The target temperatures selected for residual test conditions in this study were 23, 200, 400, 600 and 800°C.

3.4.4 Hold time

When a concrete specimen is heated in a furnace, the temperature of the furnace's air rises at a constant rate. However, the temperature of the cylinder's surface and core always rises at a slower rate than the temperature of the furnace's air. Finally, the temperature of the air reaches the target temperature significantly faster than the temperature of the cylinder.

As a result, it is necessary to maintain the furnace temperature at the target temperature for a period of time until the cylinder's core reaches the goal temperature; this period is known as hold time (or sometimes called dwell time). The method for calculating the hold time in this investigation was adapted from (Phan and Carino 2001). To track the temperature record, two thermocouples (a thermocouple is a collection of wires used to monitor temperature) were inserted in the cylinder, one in the core and the other on the surface. Type-K thermocouples were employed in this experiment. The cylinder was drilled from one of the circular ends, a thermocouple was inserted, and cement paste was grouted in the drilled section before it was cured. Figure 3.10 shows how one thermocouple was inserted on the surface. After that, a digital thermometer with thermocouples was fitted to measure their temperature (Figure 3.10). The thermocouple-embedded cylinder was then placed inside the furnace chamber, which was then heated to the desired temperature. Only the desired hold duration for heated specimens was determined by measuring the temperature track record over time for seashell high strength concrete as shown in figure 3.12.

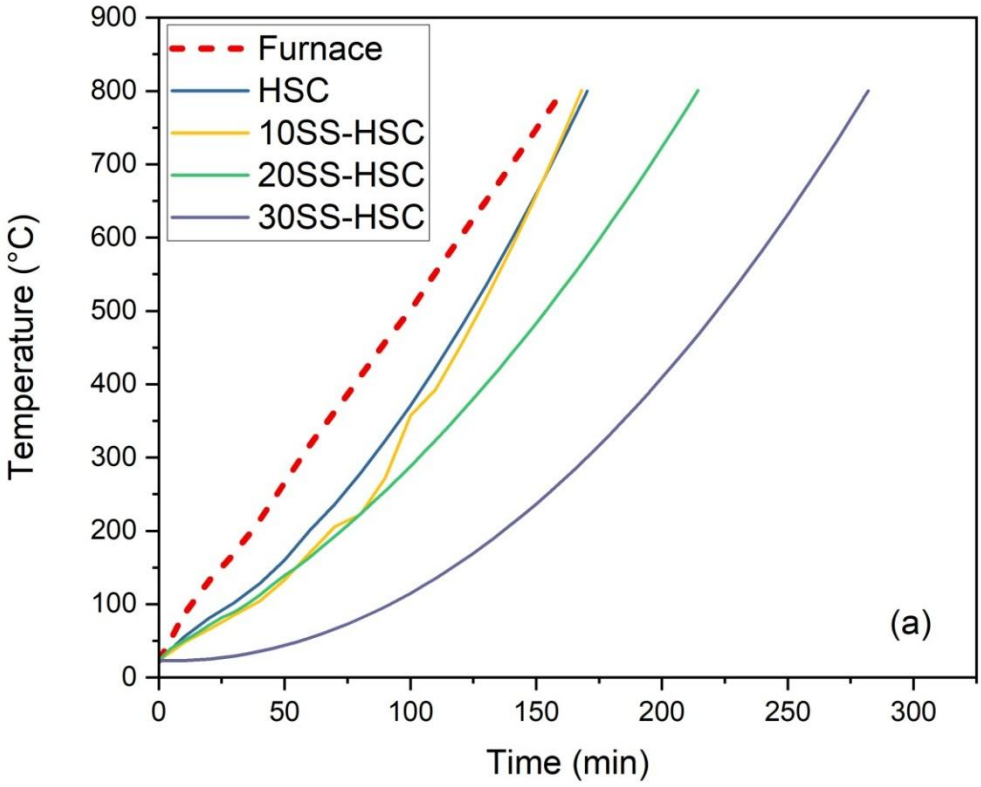

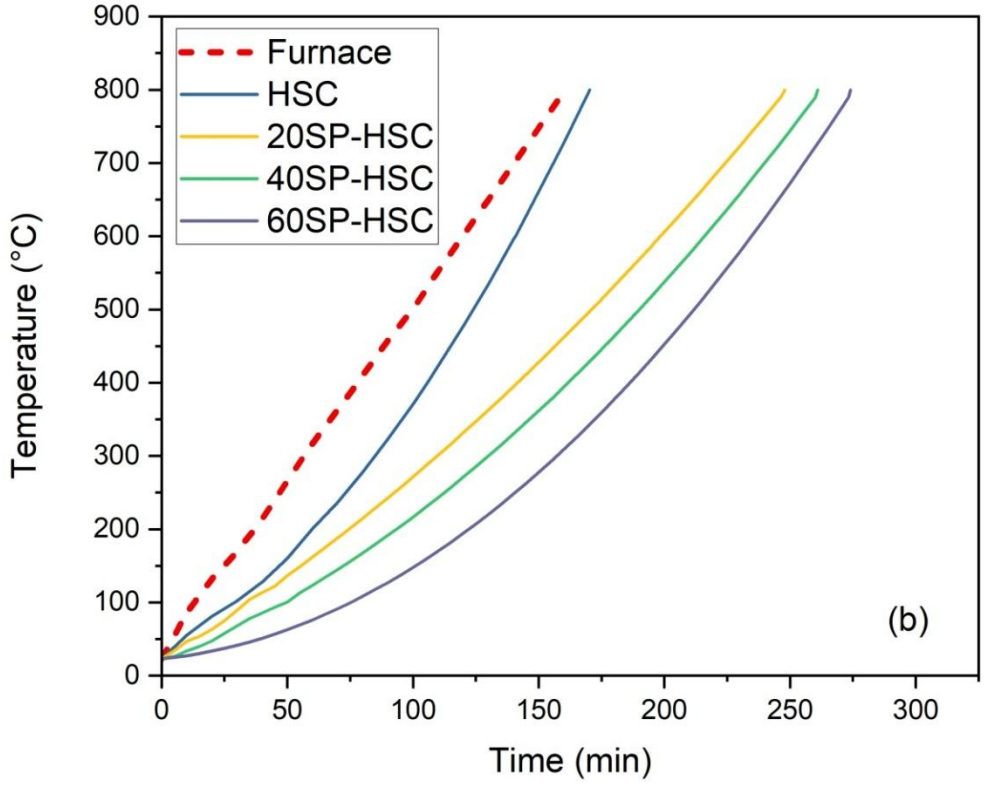

Figure 3.10 Time vs temperature curve (a) without plaster (b) with plaster

3.4.5 Heating rate

Heating rate is directly associated with spalling behavior of HSC specimens. The usual heating rate used by researchers is (2°C – 5°C)/min. A heating rate of 5°C/min was adopted in this study.

3.5 Test procedures

3.5.1 Compressive strength

Residual test conditions were used to conduct the material property test at increased temperatures. For compressive strength test, the specimen was allowed to cool to room temperature under residual test circumstances after being heated to the desired temperature up to stable thermal conditions.

Because there are no testing standards in the literature that cover high temperature compressive testing of concrete specimens, the concrete compressive strength test at target temperature (fc',T) is performed using a room temperature testing method as per the guidelines of ASTM C39/C39M-16b (Concrete and Aggregates 2014). The sample was loaded at a rate of 0.003 mm per second until the specimen failed; with a peak sensitivity of 1200 KN. Figure 3.11 depicts a concrete specimen undergoing compression testing.

One cylinder from each combination is heated and tested at a higher temperature for temperatures other than room temperature. Additional tests were performed to confirm results if they were confusing or outliers. The relative and absolute residual compressive strength of concrete specimens were estimated using the following relation to compare compressive strength by residual test condition:

$$Residual\ compressive\ strength = \frac{Residual\ strength\ at\ target\ temperature}{Room\ temperature\ strength} = \frac{f'_{c,T}}{f'_c}$$

Figure 3.11 Compression testing machine

3.5.2 Stress-strain curve

Compression tests were used to track the stress-strain response of concrete specimens using a data gathering system. The setup for a stress strain curve in compression under unstressed and residual test conditions is shown in Figure 3.11. Load and deformation data were obtained using a load data gathering system connected to a universal testing machine and LVDTs. The stress strain curve was plotted at the desired temperatures based on the load deformation response.

3.5.3 Elastic modulus

The elastic modulus of concrete specimens at target temperatures was determined using a stress-strain curve. Chord modulus according to ASTM C469/C469M-14 (2014) [89] was calculated nearest to 200 MPa by the equation shown below:

$$E_c = \frac{C_2 - C_1}{\varepsilon_2 - 0.000050}$$

Whereas,

Ec = Chord Modulus of Elasticity

$C2$ = Stress values corresponding to 0.4 fc'

$C1$ = Stress value corresponding to longitudinal strain of 0.000050

ε2 = longitudinal strain corresponding to C2

3.5.4 Mass loss

To determine the mass loss of concrete specimens, they were weighed before to heating, then heated to a desired temperature and allowed to cool to room temperature. After that, the specimens were weighed again on a weighing balance with a minimum count of 0.001 grams. The following relationship was used to compute relative mass loss at a specific temperature.

$$M_{T,loss} = \frac{Mass\ at\ target\ temperature}{Mass\ at\ room\ temperatuer} = \frac{M_T}{M}$$

Derived from mass loss test, densities were also calculated and variation in density with temperature was also monitored.

3.5.5 Strain ductility

The ability to deform after yield point is called ductility. The ductility is calculated as the ratio of strain at 80% of peak stress to the yield strain.

$$\text{Ductility} = \frac{\text{Strain at 80\% of peak stress}}{\text{Yield strain}}$$

3.6 General properties

Crack propagation, and spalling behavior were investigated as well as other features of concrete specimens that are independent of loading and heating regime. Furthermore, using traditional methodologies or procedures to present the differences in cracking patterns between two distinct concrete mixtures is ineffective.

CHAPTER 4

RESULTS AND DISCUSSIONS

4.1 Introduction

This chapter summarizes and analyses the results of tests done on concrete specimens, including mass loss, compressive strength, stress-strain response, failure mode, comparison of strain values, elastic modulus, compressive toughness, and microstructural analyses for residual test conditions. Along with checking the mechanical qualities, visual observations were taken to determine how the color and spalling behavior of all samples changed after they were removed from the electric furnace. The resulting mechanical properties data for HSC and SS-HSC with and without plaster are used to construct relationships for various material properties as a function of temperature spanning from 23 to 800 °C.

Additionally, forensic investigation of the analyzed materials was performed to determine the influence of seashell on high strength concrete subjected to elevated temperatures.

4.2 Visual assessment

In determining the serviceability of fire-damaged concrete, visual inspection is a crucial aspect. Cracking and color changes might provide a more comprehensive picture of exposure temperatures (Lau and Anson 2006, Khan, Khushnood et al. 2020). It is critical to examine the damaged structure by conducting a comprehensive study and constructing specific conclusions regarding the fire's severity, such as visible degradation, the fire's scale and spread pattern, etc (Aseem, Baloch et al. 2019). Figure 4.1 depicts the physical condition of high strength concrete and seashell modified high strength concrete (10SS-HSC, 20SS-HSC, and 30SS-HSC) after exposure to elevated temperatures. The heated samples were evaluated after being gradually cooled to room temperature.

Thermal cracking and crazing in concrete are induced principally by water loss, paste drying, and microstructure breakdown at high temperatures (Khaliq and Khan 2015). Significant fluctuation in the color of the specimens occurs in HSC samples above the exposure temperature of 200°C. The color of the specimens ranges between light grey at 200°C to grey at 400°C, and light pink at 600°C. While the temperature was growing from 600 to 800°C, spalling was detected in HSC samples.

The color of 10, 20 and 30% seashell high strength concrete was light grey at 200°C, as indicated in Figure 4.1. After 400°C exposure, the color was almost grey. The seashell concrete surface took on a pinkish color at 600°C, with no noticeable cracks. For 20 and 30% seashell concrete was become white with evident surficial fractures at 800°C. While 10% seashell concrete was spalled when temperature was start increasing from 600°C to 800°C.

Above 600°C, the spalling of HSC samples occurs, which is consistent with the literature (Kodur 2000, Khaliq 2018). HSC samples have a deep microstructure that prevents water vapors from escaping freely, resulting in a high pore pressure in the concrete matrix, causing the specimens to disintegrate and spall. The lack of spalling and lower cracking in the seashell samples implies a thermally stable behavior. The disintegration of SS particles may have resulted in the formation of a fine-pore network that is well-connected and dispersed. The existence of these pores can aid in the reduction of concrete's thermal conductivity. (Khaliq and Waheed 2017) created a thermally efficient concrete by air entrainment. These pores allow less heat to permeate the core, and the open pore system formed by SS breakdown can aid in vapor pressure dissipation.

Temp (°C)	HSC	10SS-HSC	20SS-HSC	30SS-HSC
200			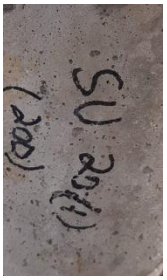	
400				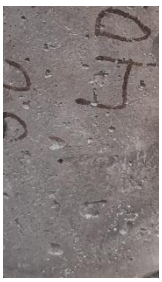

600

800

Figure 4.1 Visual assessmnet of concrete samples

4.3 Mechanical properties

4.3.1 Mass loss

Mass loss on elevated temperature is a very important factor as it removes moisture present in the matrix in different forms like free, adsorbed, absorbed, interlayer waster and capillary water. To calculate mass loss in all the samples either control or modified samples, ratio of mass at target temperature to that of ambient condition (M_T/M). Higher mass loss occurs in modified sample as shown in Figure 4.2(a). There is a phase change of moisture occurs up to 100°C from liquid to vapor state. In the temperature range of 200-800°C, modified seashell specimens lose more mass than control specimens. This is because the disintegration of seashell at high temperatures generates pores in the matrix. These pores help in dissipation of heat and will efficiently behave in crack pattern. The mass loss of HSC, 10SS-HSC, 20SS-HSC and 30SS-HSC at temperature of 400°C and 600°C are 2.11%, 3.74%, 3.89%, 4.58% and 3.64%, 5.02%, 5.26%, 5.50% respectively as compared to their mass loss at ambient temperature. This behavior clearly shows that the mass loss in HSC is less as compared to modified samples. The heat generated in HSC causes pore pressure which directly spalled the control sample at 800°C. Similarly, 10SS-HSC has less pores as compared to 20SS-HSC and 30SS-HSC and was unable to dissipate the pore pressure, hence it was also spalled at 800°C.

In Figure 4.2(b), the samples which were coated with modified plaster also show a greater loss of mass with rise in temperature as compared to control. The mass loss of HSC is lesser as compared to the modified plaster samples (20SP-HSC, 40SP-HSC, and 60SP-HSC) due to the larger pores generated in the modified plaster samples. As compared to the ambient mass loss, the mass loss for HSC, 20SP-HSC, 40SP-HSC, and 60SP-HSC are 3.64%, 9.84%, 12.10% and 24.48%, respectively at temperature 600°C. The greater mass loss in all the modified samples was because of the decomposition of seashells at high temperatures and to make a way for heat to dissipate without majorly affecting the core of the sample.

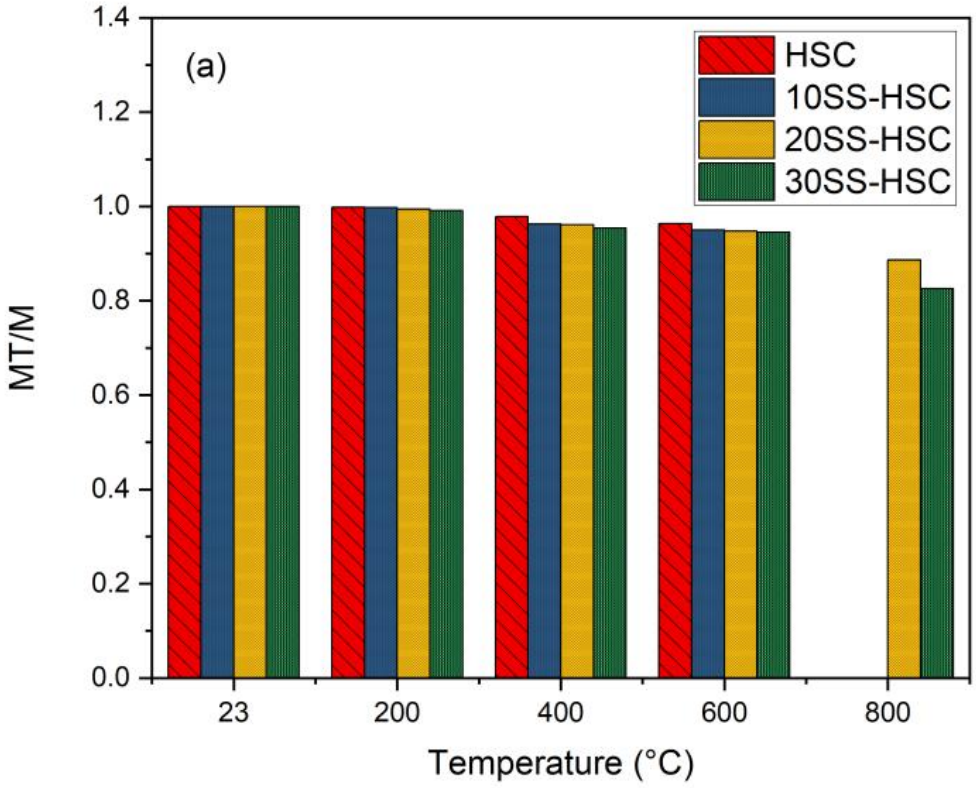

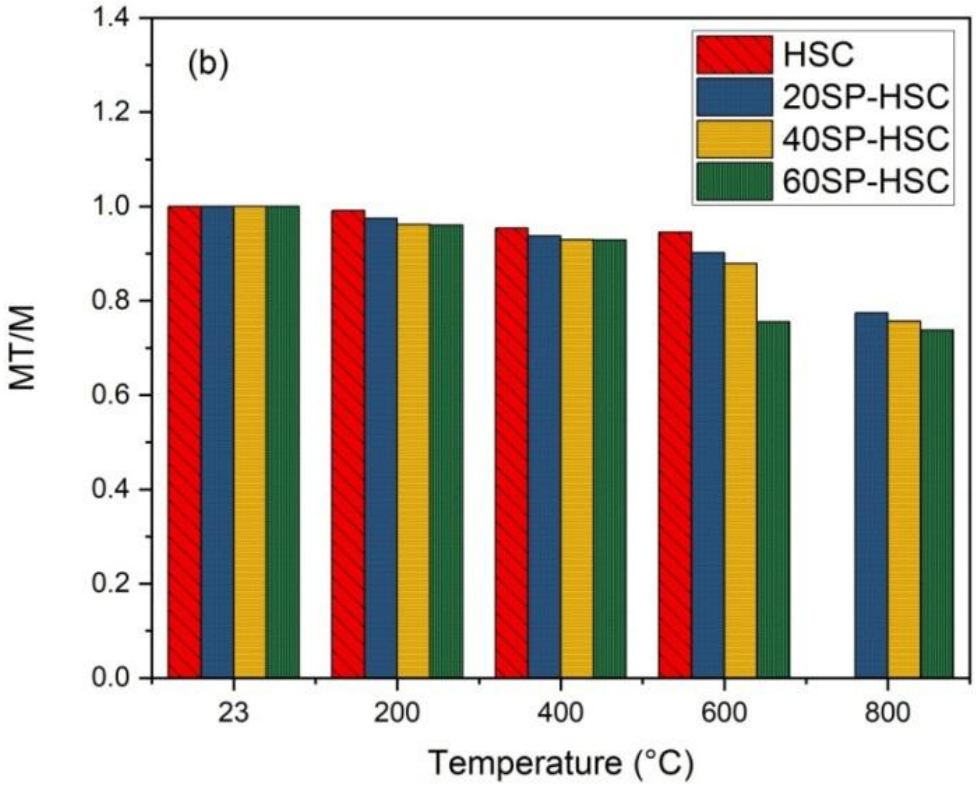

Figure 4.2 Variation in mass loss as a function of time (a) concrete without plaster (b) concrete with plaster

4.3.2 Compressive strength

The ultimate load at which specimens failed under compression was measured at various temperatures. Figure 4.3(a) shows the absolute residual compressive strength values as a function of temperature.

With increasing temperature, the declining trend was observed on all specimens, whether controls (HSC) or modified seashell HSC (10SS-HSC, 20SS-HSC, 30SS-HSC). This loss in strength is unavoidable because of the hydrothermal impact (loss of free and adsorbed water) and because concrete suffers a number of physical and chemical changes that affect its matrix when exposed to elevated temperatures (Heap, Lavallée et al. 2013). The removal of free and adsorbed water raises pore pressure to up to 200°C, resulting in micro-cracking and a loss of strength (Castillo 1987, Bažant, Kaplan et al. 1996).

Between 400 and 600°C, calcium hydroxide (Ca(OH)2) decomposes predominantly. Calcium silicate hydrate (CSH) gel decomposes at temperatures above 560°C, resulting in considerable strength loss and stiffness loss (Peng, Chan et al. 2001, Phan and Carino 2002). Above 500°C the change occurs are severe as well as unalterable (Yu and Lau 2017). In addition, thermal instability of the aggregates is the major cause of degradation at 600°C, which is due to the de-carbonation of calcium carbonate ($CaCO_3$) occur between 600 and 800°C.

The addition of seashell in HSC samples enhanced the microstructure of the specimens which ultimately increases its compressive strength with 16.71%, 27.84% and 33.31% as compared to control specimen. Seashell media present in the structure improves its microstructure by filling up the voids which enhances its compressive strength. The strength loss of control sample was very much noticeable between 200 and 800°C, beyond 600°C it was spalled. However, the modified samples with seashell show much better retention of strength as compared to control specimen. The sample with 30% replacement showed the highest strength retention due to the highest thermally resistant material used in the mix.

At 100°C, physical connected water was lost in the cement matrix. The cracks formed as a result of pore pressure and its evacuation from the concrete. Because of the formation of cracks, the effective load bearing area decreases, resulting in a decrease in strength. The compressive strength loss is dormance up to 200°C in all the samples but show increase of 10.34%, 20.70% and 58.12% of modified samples as compared to control. Up to 400°C, less retention of compressive strength occurs for modified samples as compared to HSC. Because there are fewer pores in seashell modified up to 400°C that causes greater loss of strength. Between 400°C-600°C, there is a lesser strength loss of 58.57% in 30SS-HSC as compared to 73.92% in HSC. This behavior of seashell shows that the seashell decomposes when the temperature exceeds 400°C. Therefore, this decomposition developed micro-pores which resultantly help in dissipation of pore pressure. These pores help in two ways i.e., they dissipate vapor pressure and reduce the matrix's total thermal conductivity. Above 800°C, HSC and 10SS-HSC samples were spalled while 20SS-HSC and 30SS-HSC were show better retention in strength. This retention of strength showed that seashell is thermally stable material.

In Figure 4.3(b), the specimens of HSC coated with modified seashell mortar have been shown greater strength as compared to control specimen on ambient temperature. Because of lesser pores generated in the seashell samples the loss of strength of all the specimens up to 400°C was almost similar. The pores generated in seashell sample above 400°C, efficiently dissipate vapor pressure which resultantly greater retention in strength. At 600°C, the loss of strength at 60SP-HSC was 61.52% as compared to 73.92% in HSC. The results showed that, seashell mortar specimens at 800°C were exceptionally good in retaining the strength as compared to control specimen. This improved behavior of seashell mortar is due to the pores generated in the matrix when exposed to higher temperature which reduces the spalling of the sample. The results show that plastering technique is very much efficient in resisting the structure against fire.

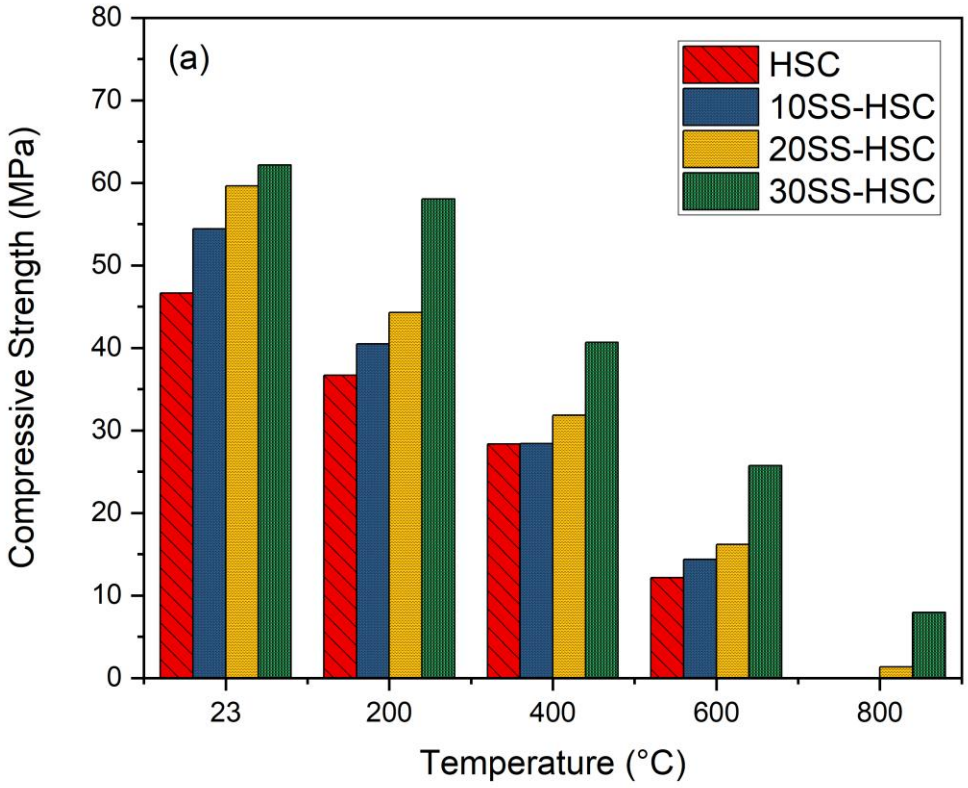

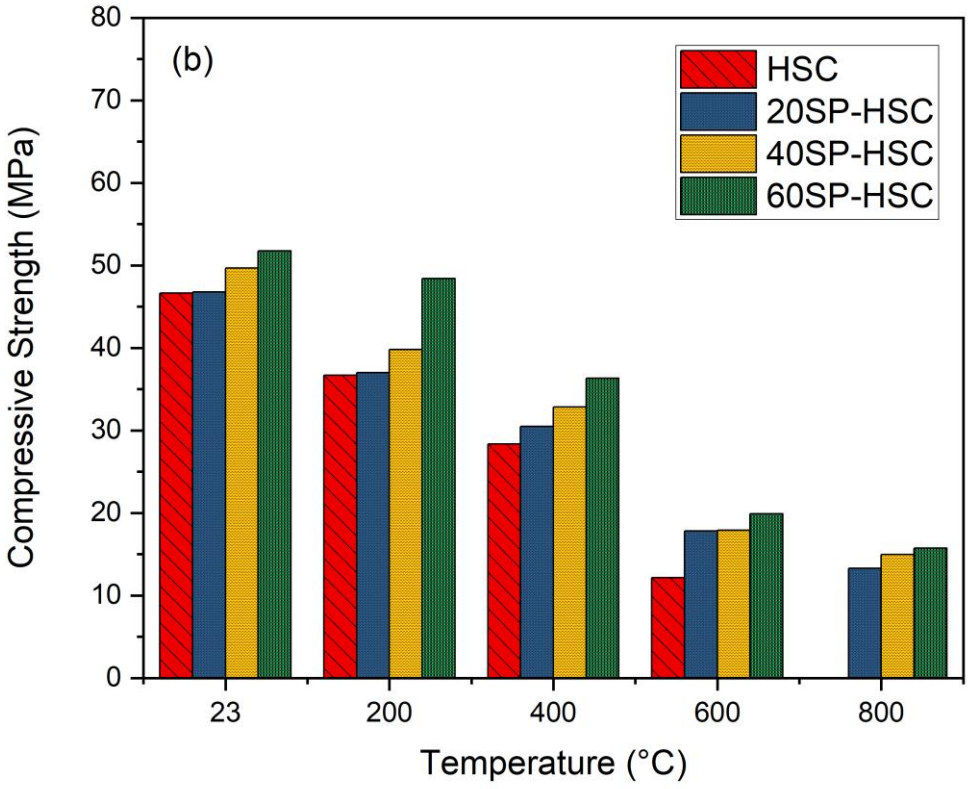

Figure 4.3 Absolute residual compressive strength of concrete values as a function of temperature (a) without plaster (b) with plaster

4.3.3 Stress-strain response

Stress-strain response of control HSC and modified HSC (10SS-HSC, 20SS-HSC and 30SS-HSC) were assessed from compression test and Figure 4.4 shows these stress-strain curves were plotted against temperatures for residual test conditions. From 23 to 400°C, all the specimens show that with the increase in temperature the values of peak stress were decreased with the decrease in the corresponding strains. Above 400°C temperature, the strain values were increased with the decrease in peak stress was aforementioned in the literature (Phan 2002, Khaliq and Kodur 2011, Khaliq 2012).

The Figure 4.4(a) shows that the seashell modified sample has greater compressive strength of 62.16MPa with greater strain value of 0.00238396 as compared to control. These greater values of stress are due to the more packing density of seashell modified samples at ambient temperature. This trend was similar for the temperature of 200°C (Figure 4.4(b)) and 400°C (Figure 4.4(c)). Further increase in temperature to 600°C, the stress value of 20SS-HSC was 16.17MPa with strain value of 0.00215681 which is smaller than control specimen as shown in Figure 4.4(d). Further increase in temperature to 800°C in Figure 4.4(e), HSC and 10SS-HSC was spalled because of lesser pores in the matrix. But 30SS-HSC has lesser strain value of 0.00298472 as compared to 0.0033041 for 20SS-HSC. This behavior of modified seashell samples is due to an open pore system in the seashell modified high strength concrete. The results show that open pore system is a result of seashell decomposition. Pores generated in the matrix are helpful in dissipation of vapor pressure which directly reduced the cracks potential and less damage to cross-sectional areas. Pores development and decreased in strains in the modified samples at higher temperatures is directly related to less deterioration because seashell in the concrete matrix deviate the crack trajectory. (Khaliq and Waheed 2017) also investigated this behavior of fire resistance of concrete with entrained air voids

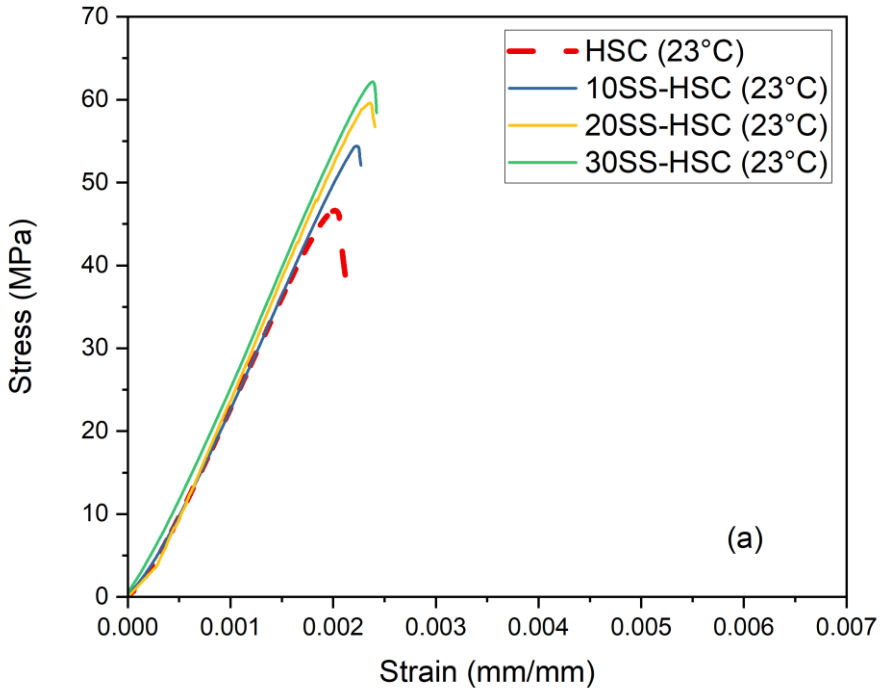
HSC (23°C)
10SS-HSC (23°C)
20SS-HSC (23°C)
30SS-HSC (23°C)
(a)
Stress (MPa)
Strain (mm/mm)
0
10
20
30
40
50
60
70
0.000
0.001
0.002
0.003
0.004
0.005
0.006
0.007

.

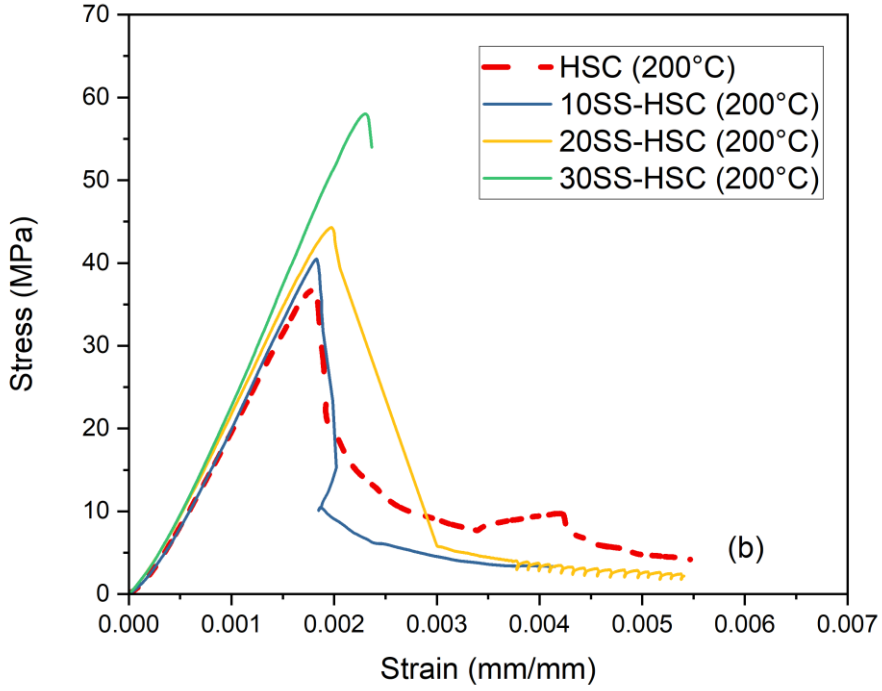
HSC (200°C)
10SS-HSC (200°C)
20SS-HSC (200°C)
30SS-HSC (200°C)
(b)
Stress (MPa)
Strain (mm/mm)
0
10
20
30
40
50
60
70
0.000
0.001
0.002
0.003
0.004
0.005
0.006
0.007

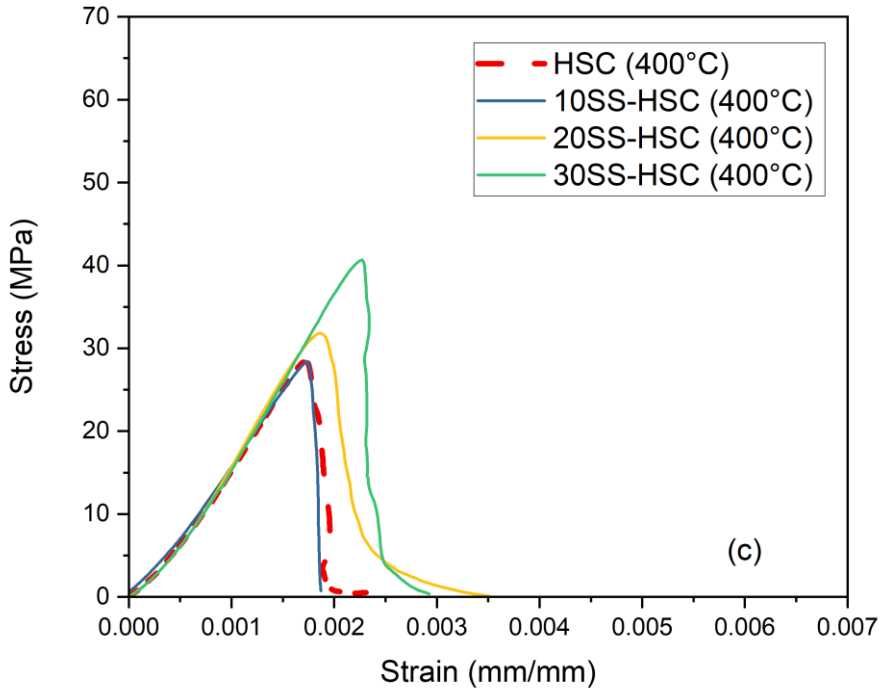
HSC (400°C)
10SS-HSC (400°C)
20SS-HSC (400°C)
30SS-HSC (400°C)
(c)
Stress (MPa)
Strain (mm/mm)
0
10
20
30
40
50
60
70
0.000
0.001
0.002
0.003
0.004
0.005
0.006
0.007

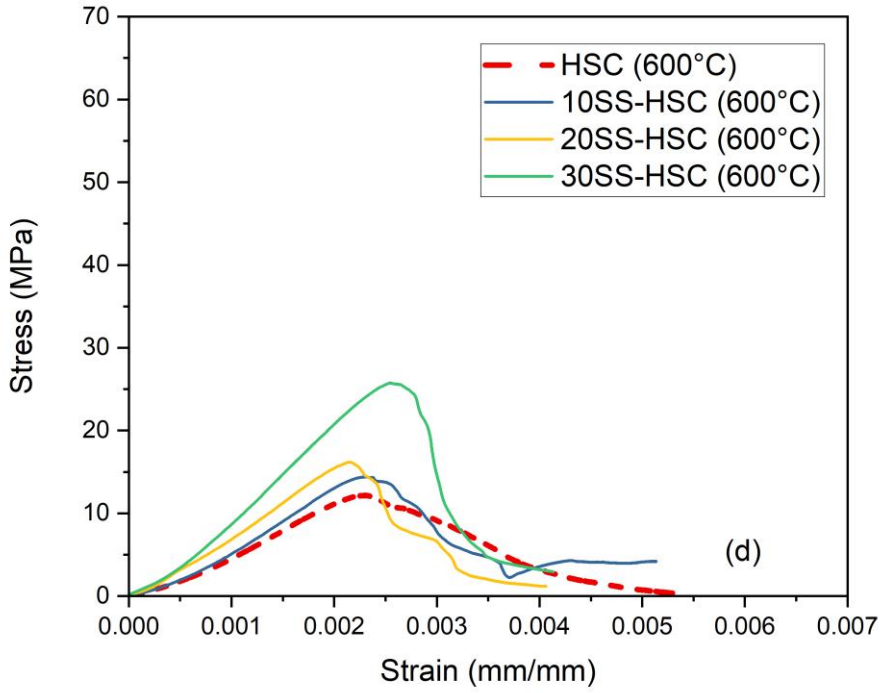
HSC (600°C)
10SS-HSC (600°C)
20SS-HSC (600°C)
30SS-HSC (600°C)
(d)
Stress (MPa)
Strain (mm/mm)
0
10
20
30
40
50
60
70
0.000
0.001
0.002
0.003
0.004
0.005
0.006
0.007

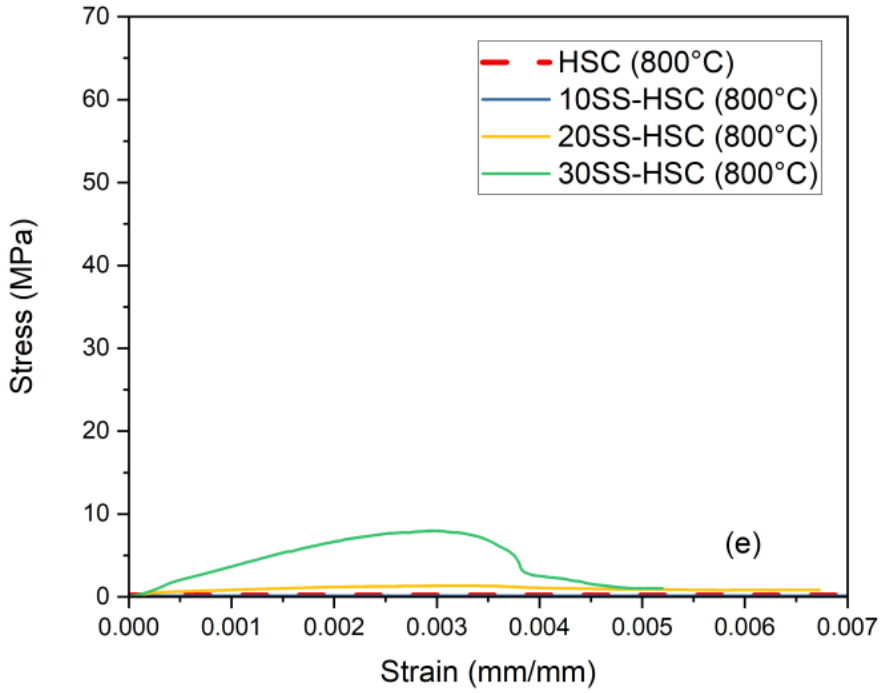

Figure 4.4 Stress-strain at ambient and elevated temperature (a) 23°C (b) 200°C (c) 400°C (d) 600°C (e) 800°C

4.3.4 Failure mode

All the samples either control or modified seashell sample show a brittle failure at ambient temperature as shown in Figure 4.5. Although modified seashell samples were showed more brittle nature because of their dense microstructure at ambient temperature. But with the increase in temperature, brittle nature of sample becomes converted to some extent stable. The samples at 200°C showed larger cracks, the behavior was brittle with abrupt failure. It was observed that relatively lesser cracks were developed at 400°C. With further increase in temperature upto 600°C, the cracks were proportionally reduced. At an extreme temperature of 800°C, HSC and 10SS-HSC disintegrated completely while external surface of 20SS-HSC and 30SS-HSC got defected. Cracking was observed but the core did not disintegrated due to pores developed in the sample which ultimately intact the sample. All the samples especially seashell modified samples above 200°C have lesser cracks shown because of the disintegration of the matrix causes voids and were reduced the brittle nature of the concrete.

Temp (°C)	HSC	10SS-HSC	20SS-HSC	30SS-HSC
23				
200				
400				
600				

800 

Figure 4.5 Failure modes of concrete samples on all temperatures

4.3.5 Comparison of strain values

A comparison of all the samples was made with the increase in temperature. The value of yield strain, peak strain and ultimate strain of HSC was shown in Figure 4.6(a). The yield strain values up to 400°C decreased with the increased in temperature. The yield strain values were decreased to 12.04% at 400°C temperature. The peak and ultimate strains of the HSC were also decreased up to 400°C. Because of the dense structure of HSC and has the ability to resist temperature. For 600°C, the ultimate strain of the HSC was increased to 34.08% as compared to ambient strain. This behavior is due to the large temperature causes larger deterioration in the sample which causes greater strain values on lower stress values. At 800°C, the strain values were not captured as the sample was spalled because of the extreme deterioration in the sample.

The comparison of strain values of 10SS-HSC are shown in Figure 4.6(b). The yield strain values decreased with the increase in temperature up to 400°C. This is due to the dense structure causes less deterioration in the matrix. For 600°C, there is an increase of 1.6% in the yield strain values. The ultimate and peak strain values are also increase at 600°C. This behavior of 10SS-HSC is due to greater cracks in the matrix causes large deterioration and has larger strain values. The strain values at 800°C were not captured because there was a large deterioration in the matrix caused spalling of the sample

The strain values for the sample 20SS-HSC are shown in Figure 4.6(c). The peak strain values were decreased up to 400°C and show increasing trend at 600 and 800°C. This behavior was due to the less cracks developed in the matrix up to 400°C and the cracks were increased at higher temperature causes more deterioration. The ultimate and yield strain didn't give similar trend on 800°C because the cracks were very large which causes large deterioration and were not give proper trend.

Figure 4.6(d) shows the comparison of strain values of 30SS-HSC. The peak strain values decreased 4.9% up to 400°C. Above 600°C, there is rise in peak strain values. At 800°C, the increase in peak strain value of 25.2% as compared to ambient peak strain. The strain were increased due to the large cracks developed on higher temperatures causes more deterioration. The yield strain were not properly captured because of the more cracks developed in the matrix. The ultimate strain was increased to 47.33% which is due to larger cracks developed and the material show less brittle failure at higher temperatures.

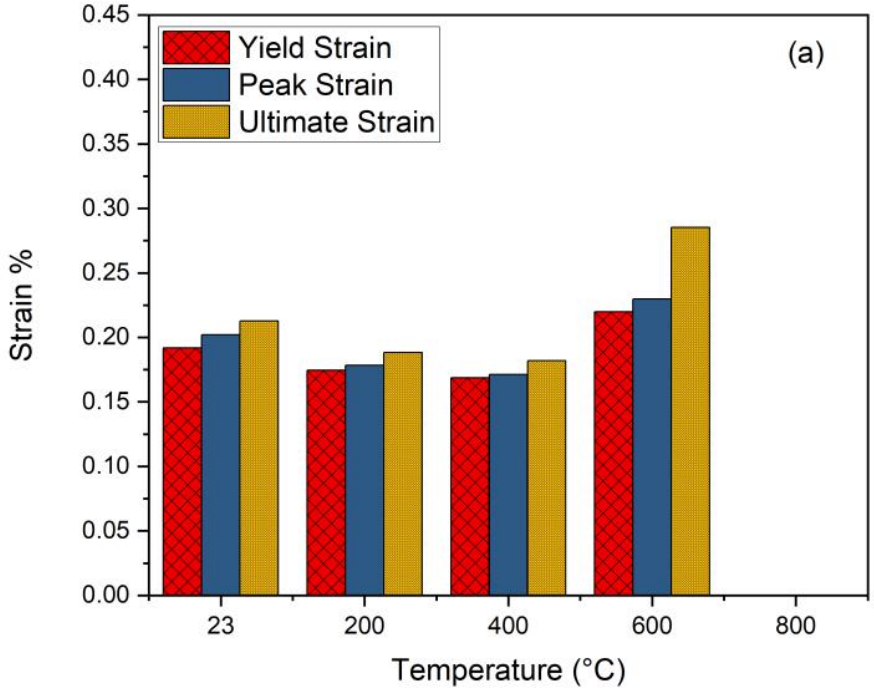
Yield Strain
Peak Strain
Ultimate Strain
(a)
Strain %
0.45
0.40
0.35
0.30
0.25
0.20
0.15
0.10
0.05
0.00
23
200
400
600
800
Temperature (°C)

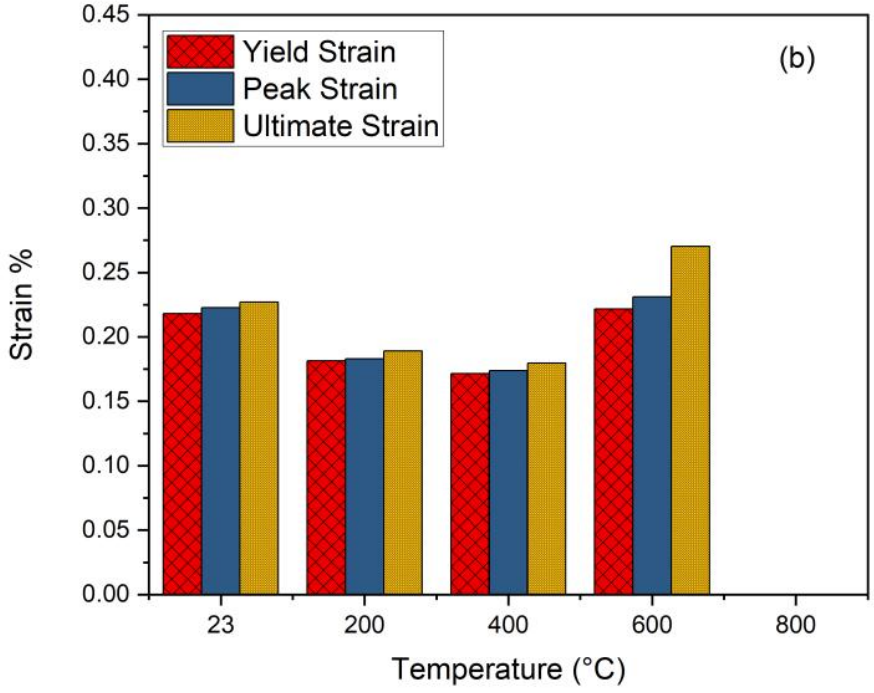
Yield Strain
Peak Strain
Ultimate Strain
(b)
Strain %
0.45
0.40
0.35
0.30
0.25
0.20
0.15
0.10
0.05
0.00
23
200
400
600
800
Temperature (°C)

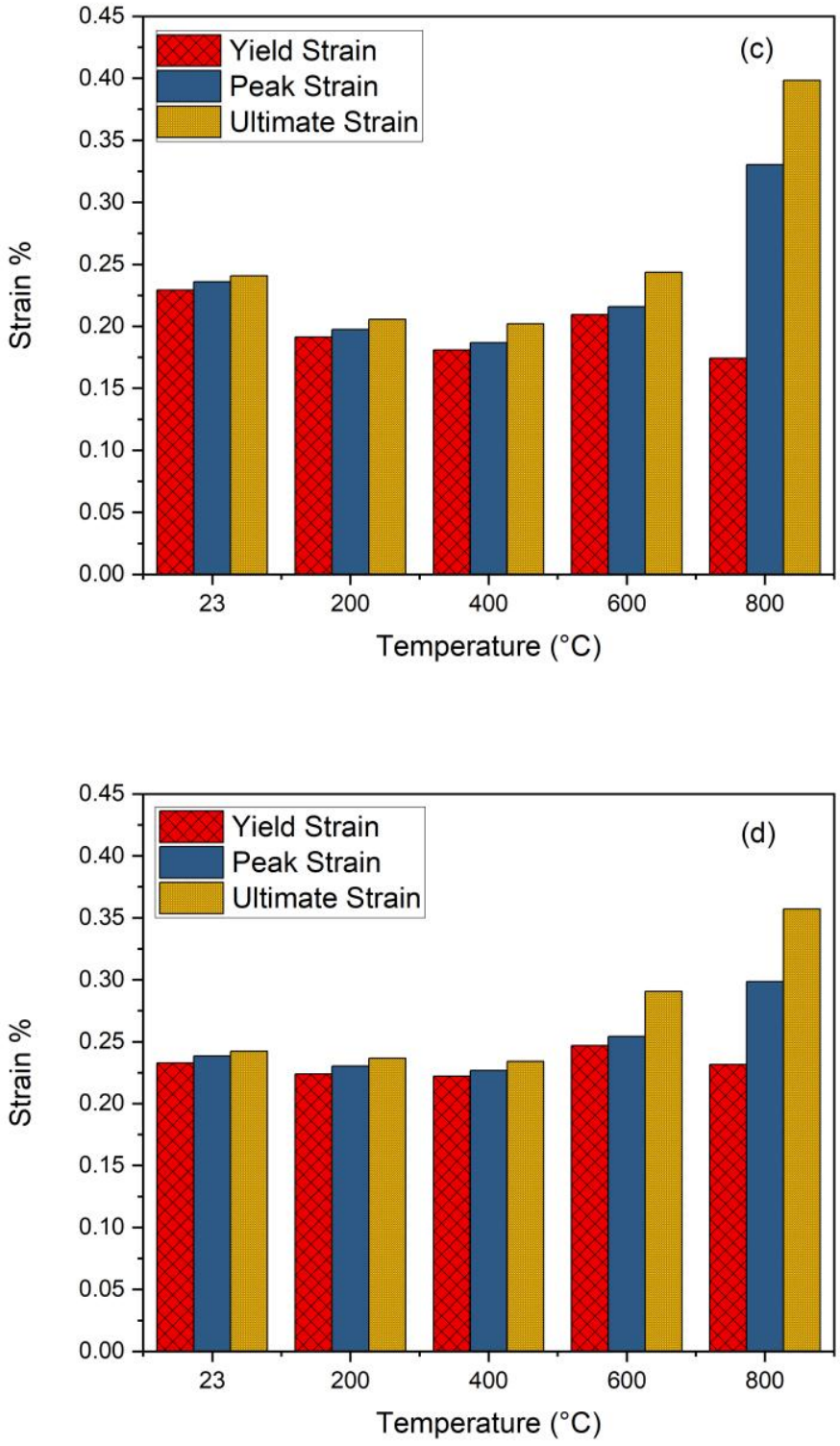

Figure 4.6 Strain values for (a) control HSC (b) 10SS-HSC (c) 20SS-HSC (d) 30SS-HSC

4.3.6 Elastic modulus

Stress-strain curve is utilized for determining elastic modulus for both control and modified seashells HSC samples. The strain at 40% of stress value is utilized to calculate secant modulus of all the formulations. In the residual state condition, the absolute elastic moduli of the studied formulations are illustrated in Figure 4.7. The results show that the modified seashell samples have greater retention of elastic modulus as compared to control sample at targeted temperatures. The elastic modulus of 10SS-HSC, 20SS-HSC and 30SS-HSC at 600°C has smaller loss of 76.28%, 71.38% and 63.78%, respectively as compared to 79.11% in control HSC.

This retention is due to the pore pressure generated in the matrix was decremented by decomposition of seashell and it would efficiently behave in maintaining the elastic modulus. The behavior of HSC is evident from the literature that by loss in mechanical strength, elastic modulus was also compromised (Phan, Lawson et al. 2001).

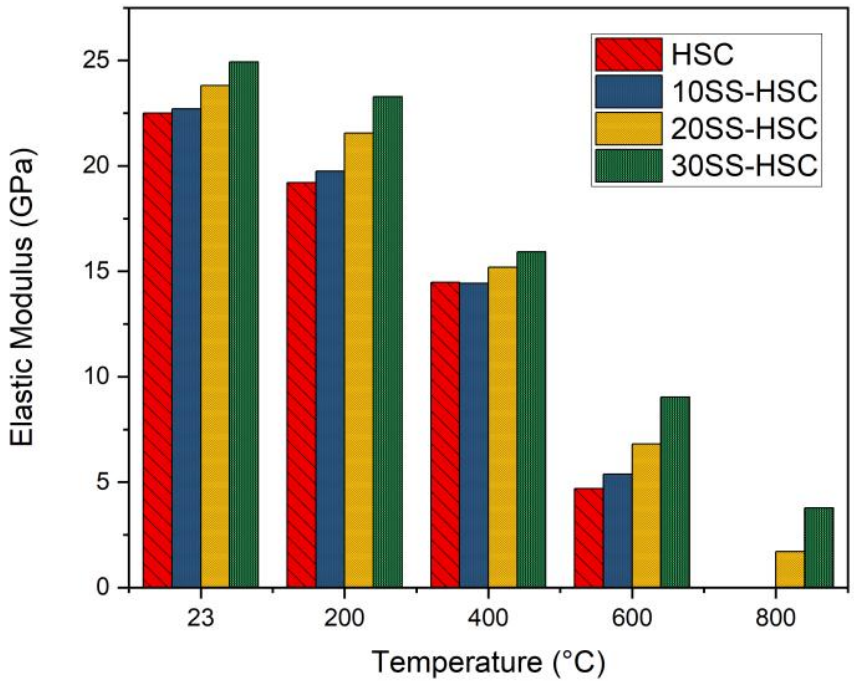

Figure 4.7 Elastic modulus as a function of time

4.3.7 Strain ductility

Important characteristic is to determine the ductility of the specimens, which is the ability to deform after yield point. The ductility is calculated as the ratio of strain at 80% of peak stress to the yield strain.

The ductility was computed on the basis of rise in temperature, with the increase in temperature the ductility of the sample increases. From Figure 4.8 shows, the ductility of the control sample at the temperature of 600°C was 1.29 which is more than the 1.10 at its ambient temperature. The ductility of 10SS-HSC at 600°C was calculated as 1.21 which is greater than 1.04 at its ambient condition. The 20SS-HSC showed that greater ductile value of 2.28 at 800°C as compared to 1.04 at ambient temperature. However, 30SS-HSC show the same trend as 1.54 ductile value at 800°C as compare to lesser value of 1.04 at ambient temperature. This behavior of ductility is just depending on the temperature rise as with the increase in temperature there are pores generated in the sample which directly delay the abrupt failure after peak load.

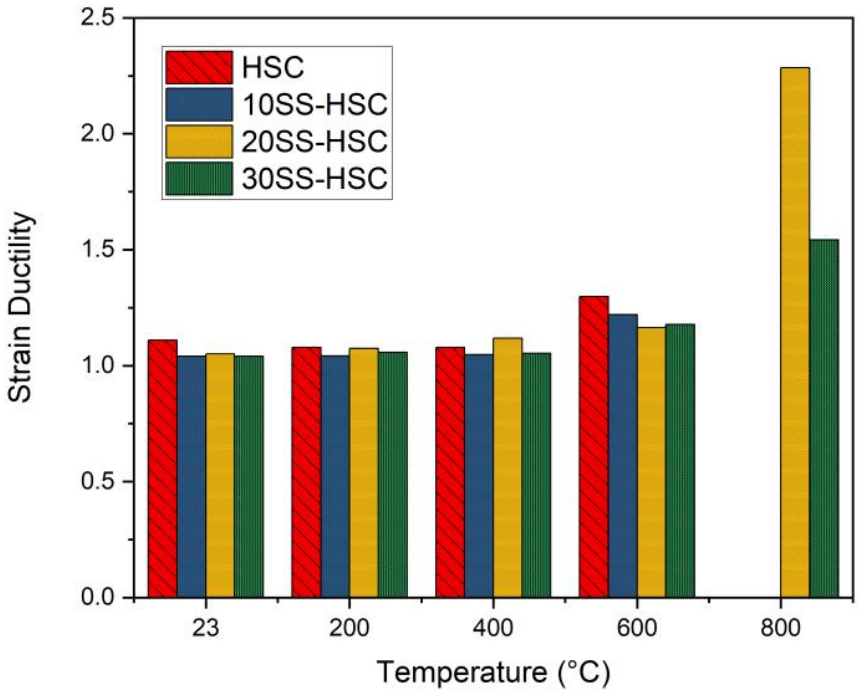

Figure 4.8 Strain ductility values comparison for specimens

4.3.8 Total crack energy absorb in compression (TEC) or compressive toughness

Compressive toughness (T_C) is calculated by calculating the area under the stress-strain curve up to the 20% drop in peak stress, which measures concrete energy absorption before failure and its ability to resist deformation under compression. Ultimate strain value limit is based on the previous studies (Marar, Eren et al. 2001, Marara, Erenb et al. 2011). The Energy absorption values was calculated and were plotted against targeted temperatures for all the specimens (HSC, 10SS-HSC, 20SS-HSC and 30SS-HSC) as shown in Figure 4.9. At all the targeted temperatures, there was an increasing trend of energy absorption. At ambient temperature, results show that total absorb energy for HSC is 0.05153 is lesser as compared to the 0.06078, 0.07147 and 0.0765 for 10SS-HSC, 20SS-HSC and 30SS-HSC, respectively. The results show that by addition of seashell at all targeted temperatures there is an increase of energy absorption (toughness). Because there is a greater value of peak stress for 10SS-HSC, 20SS-HSC and 30SS-HSC as compared to the control specimen. This tougher behavior of modified seashells may also due to its ability to resist at elevated temperatures because of the pores generation in result of seashell disintegration.

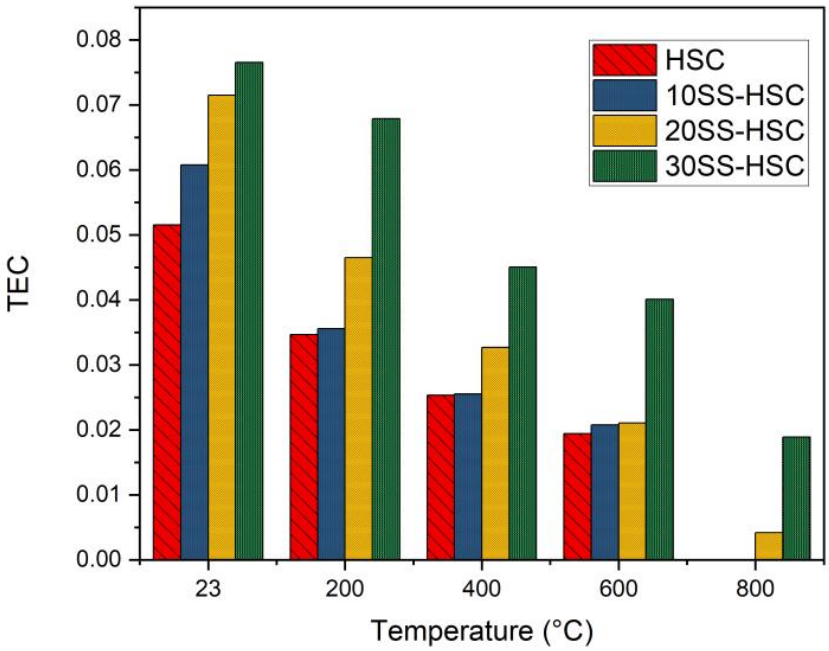

Figure 4.9 Compressive toughness as a function of temperature

4.3.9 Pre-crack energy absorb in compression (PEC)

Area under the stress-strain curve from start point to the yield point is defined as pre-crack energy. The pre-crack energy was increased as the percentages of the sample were increased. The modified samples have greater pre-crack energy as compared to the control sample as shown in Figure 4.10. The 30SS-HSC shows greater pre-crack energy of 0.07063 at ambient temperature. The similar trend was shown at all the targeted temperatures. Similarly, at 600°C the pre-crack energy of 30SS-HSC was 0.02936 as compared to the control sample of 0.01213. The increase in pre-crack energy for modified sample at higher temperatures is due to the high pores generation, which dissipates heat resulting in higher yield point values.

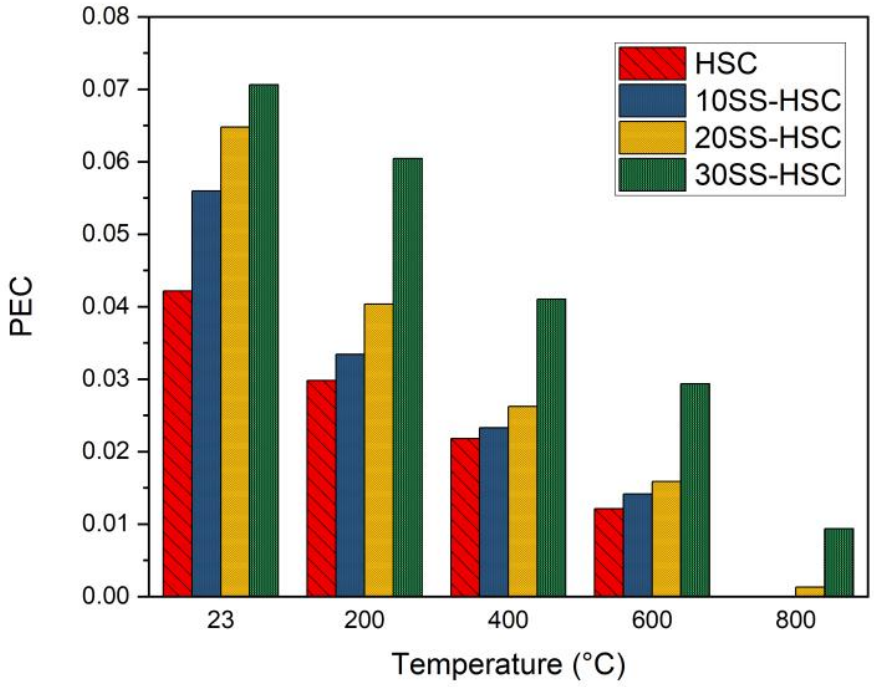

Figure 4.10 PEC values comparison for specimens as a function of temperature

4.3.10 Toughness index (TI)

Toughness index is the ratio of increase or decrease in the modified seashell HSC sample to the control sample at targeted temperatures.

$$TI = \frac{Tc \text{ of seashell modified concrete samples at targeted temperature}}{Tc \text{ of control samples at target temperature}}$$

Fig. 4.11, show the toughness index of all the formulations. Base line represents the control specimen from which the increase or decrease in the toughness can be identified for all the modified samples. In the temperature range between 23 to 200°C the toughness index for all the modified samples are greater than the control one. The trend was similar for all the modified samples as they have increment in toughness index of 17.95, 38.69 and 48.49 as compared to control specimen for ambient condition. At the temperature of 200°C the similar increasing trend of toughness index for modified sample was shown with increase of 2.63%, 34.24% and 95.92% respectively as compared to control specimen. At the temperature of 400°C and 600°C also show an increasing trend in modified samples for toughness up to 0.83%, 29.10%, 77.97% and 6.79%, 8.29%, 106% respectively. This behavior of toughness index indicates that the seashell in the matrix of sample have improvement in deformability and fracture resilience. Effectively dissipation of vapors pressure in seashell modified sample helps in improvement of immediate fracture. The cavities developed in the matrix are helpful in deviation of crack trajectory and was helpful in addition in fracture energy.

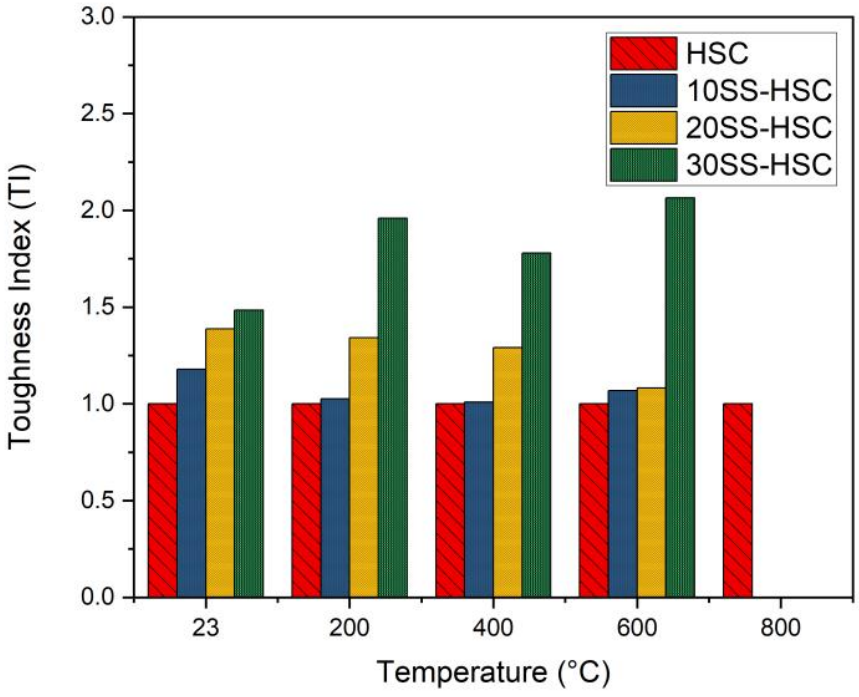

Figure 4.11 Toughness index as function of temperature

CHAPTER 5

CONCLUSIONS AND RECOMMENDATIONS

5.1 Conclusions

Following conclusion are presented on basis of analysis of results obtained from this experimental work:

- In visual assessment, there are surficial cracks present on the samples above 400°C for HSC and modified HSC either with plaster or without plaster coating. However, there was no spalling occurred in any of the plaster sample. The HSC and 10SS-HSC spalled above 600°C, although 20SS-HSC and 30SS-HSC were not spalled. The cracks present on the modified samples were relatively lesser than the control samples.
- The mass loss for seashell samples either with plaster or without plaster samples were higher than the control samples. This phenomenon was caused by the disintegration of seashells at high temperatures and the need to release heat without harming the sample's core.
- Seashell modified (with or without plaster) samples shows higher residual compressive strength at elevated temperature with relatively better spalling sensitivity. This identifies the better pore distribution system of seashell HSC, which creates micro-pores due to decomposition of seashells. The findings indicate that the plastering technique is more effective in fire resistance.
- The stress-strain responses of seashell modified samples are much better than the control samples at elevated temperature. The findings demonstrate that the open pore system is caused by the disintegration of seashells. Pores formed in the matrix aid in the dissipation of vapor pressure, reducing the risk of cracking and causing less damage to cross-sectional regions. At higher temperatures, the development of pores and an increase in stresses is directly proportional to less breakdown of the concrete matrix.
- All the samples either control or modified seashell sample demonstrate a brittle failure at ambient temperature. But the rise in temperature shows lesser brittle behavior as compared to ambient temperatures and the failure was not abrupt.

- The strain values for all the samples decreased up to 400°C because of the dense structure causes less deterioration in the matrix. Above 600°C temperature, strain values have been increased due to greater cracks in the matrix causes large deterioration.
- When compared with the control specimen, the elastic modulus for the modified samples has more retention due to the lesser pore pressure generation. This behavior is due to the seashells, those have a helpful character that aids in reduced thermal breakdown in the matrix.
- All the samples show improvement in the ductility due to rise in temperature. However, the energy absorption capacities of the samples were enhanced because of the higher peak point as well as the effective heat dissipation of the seashell samples. This shows that the modified samples were tougher than the control samples.

5.2 Recommendations

- This study was focused on the mechanical properties of seashell high strength concrete with plaster and without plaster at elevated temperatures.
- Further study can be done to achieve optimum percentage of seashell in concrete under compression test for ambient as well as on elevated temperature.
- The structural members made up of seashell concrete, thermal and mechanical properties of seashell high strength concretes in both unstressed and stressed conditions.
- Flexural behavior of concrete at elevated temperature by using various percentages of seashells can be evaluated.

REFERENCES

A. (2013). "CT-13 ACI Concrete Terminology." ACI Materials Journal.

Abeer, S., et al. (2020). "Investigation some properties of recycled lightweight concrete blocks as a fine aggregate in mortar under elevated temperature." Periodicals of Engineering and Natural Sciences (PEN) **8**(1): 400-412.

Akca, A. H. and N. Ö. Zihnioğlu (2013). "High performance concrete under elevated temperatures." Construction and Building Materials **44**: 317-328.

Al-Akhras, N. M., et al. (2009). "Performance of olive waste ash concrete exposed to elevated temperatures." Fire Safety Journal **44**(3): 370-375.

Ali, F., et al. (2001). "Explosive spalling of high-strength concrete columns in fire." Magazine of Concrete Research **53**(3): 197-204.

Anderberg, Y. (1997). Spalling phenomena of HPC and OC. NIST Workshop on Fire Performance of High Strength Concrete in Gaithersburg.

Aseem, A., et al. (2019). "Structural health assessment of fire damaged building using non-destructive testing and micro-graphical forensic analysis: A case study." Case Studies in Construction Materials **11**: e00258.

Astm, A. (2015). "C617/C617M 15–standard practice for capping cylindrical concrete specimens." ASTM American Society for Testing and Materials–Committee C09 on Concrete and Concrete Aggregates–Subcommittee C **9**.

ASTM, A. (2017). "C150/C150M-17, Standard Specification for Portland Cement." American Society for Testing and Materials: West Conshohocken, PA, USA.

Awal, A. A., et al. (2015). "Effect of cooling regime on the residual performance of high-volume palm oil fuel ash concrete exposed to high temperatures." Construction and Building Materials **98**: 875-883.

Bamigboye, G., et al. (2021). "Mechanical and durability assessment of concrete containing seashells: A review." Cogent Engineering **8**(1): 1883830.

Barnett, S., et al. (2004). "Fast-track concrete construction using cement replacement materials." Special Publication **221**: 135-152.

Bastami, M., et al. (2011). "Performance of high strength concretes at elevated temperatures." Scientia Iranica **18**(5): 1028-1036.

Bažant, Z. P., et al. (1996). "Concrete at high temperatures: material properties and mathematical models."

Bijen, J. (1996). "Blast furnace slag cement for durable marine structures. Stichting Beton Prima." Amsterdam: Elservier.

C33, A. (2003). "ASTM C33 standard specifications for concrete aggregates." ASTM Standard Book.

C1231/C1231M-12 "A.C.M.-. Practice for Use of Unbonded Caps in Determination of Compressive Strength of Hardened Concrete Cylinders.".

Carino, N. (1994). "Effects of testing variables on the strength of high-strength (90 MPa) concrete cylinders." Special Publication **149**: 589-632.

Castillo, C. (1987). Effect of transient high temperature on high-strength concrete, Rice University.

Castillo, C. and A. Durrani (1990). "Effect of transient high-temperature on high-strength concrete-closure." ACI Materials Journal **87**(6): 653-653.

Chan, Y., et al. (1999). "Residual strength and pore structure of high-strength concrete and normal strength concrete after exposure to high temperatures." Cement and Concrete Composites **21**(1): 23-27.

Chandra, S. and L. Berntsson (2002). Lightweight aggregate concrete, Elsevier.

Cheng, F.-P., et al. (2004). "Stress-strain curves for high strength concrete at elevated temperatures." Journal of Materials in Civil Engineering **16**(1): 84-90.

Committee, A. (2008). Guide for selecting proportions for high-strength concrete using Portland cement and other cementitious materials, American Concrete Institute.

Concrete, A. I. C. C. o. and C. Aggregates (2014). Standard test method for compressive strength of cylindrical concrete specimens, ASTM international.

Demir, I., et al. (2011). "Performance of cement mortars replaced by ground waste brick in different aggressive conditions." Ceramics-Silikáty **55**(3): 268-275.

Duval, R. and E. Kadri (1998). "Influence of silica fume on the workability and the compressive strength of high-performance concretes." Cement and Concrete Research **28**(4): 533-547.

Ergün, A., et al. (2013). "The effect of cement dosage on mechanical properties of concrete exposed to high temperatures." Fire Safety Journal **55**: 160-167.

Evart, B. (2018). "Fire Loss In The United State During 2017, Natl. Fire Prot. Assoc. ."

Felicetti, R., et al. (2013). "Thermal and mechanical properties of light-weight concrete exposed to high temperature." Fire and materials **37**(3): 200-216.

Georgali, B. and P. Tsakiridis (2005). "Microstructure of fire-damaged concrete. A case study." Cement and Concrete Composites **27**(2): 255-259.

Han, C.-G., et al. (2005). "Performance of spalling resistance of high performance concrete with polypropylene fiber contents and lateral confinement." Cement and Concrete Research **35**(9): 1747-1753.

Heap, M., et al. (2013). "The influence of thermal-stressing (up to 1000 C) on the physical, mechanical, and chemical properties of siliceous-aggregate, high-strength concrete." Construction and Building Materials **42**: 248-265.

Hoff, G. C., et al. (2000). "Elevated temperature effects on HSC residual strength." Concrete International **22**(4): 41-48.

Hora, M., et al. (2013). "Temperature analysis of lightweight aggregate concrete slab members at elevated temperatures for predicting fire resistance." Applications of Structural Fire Engineering.

Horszczaruk, E., et al. (2017). "The effect of elevated temperature on the properties of cement mortars containing nanosilica and heavyweight aggregates." Construction and Building Materials **137**: 420-431.

Husem, M. (2006). "The effects of high temperature on compressive and flexural strengths of ordinary and high-performance concrete." Fire Safety Journal **41**(2): 155-163.

Janotka, I. and T. Nürnbergerová (2005). "Effect of temperature on structural quality of the cement paste and high-strength concrete with silica fume." Nuclear Engineering and Design **235**(17-19): 2019-2032.

Kalifa, P., et al. (2000). "Spalling and pore pressure in HPC at high temperatures." Cement and Concrete Research **30**(12): 1915-1927.

Khaliq, W. (2012). Performance characterization of high performance concretes under fire conditions.

Khaliq, W. (2018). "Mechanical and physical response of recycled aggregates high-strength concrete at elevated temperatures." Fire Safety Journal **96**: 203-214.

Khaliq, W. and H. A. Khan (2015). "High temperature material properties of calcium aluminate cement concrete." Construction and Building Materials **94**: 475-487.

Khaliq, W. and V. Kodur (2011). "Thermal and mechanical properties of fiber reinforced high performance self-consolidating concrete at elevated temperatures." Cement and Concrete Research **41**(11): 1112-1122.

Khaliq, W. and F. Waheed (2017). "Mechanical response and spalling sensitivity of air entrained high-strength concrete at elevated temperatures." Construction and Building Materials **150**: 747-757.

Khan, E. U., et al. (2020). "Spalling sensitivity and mechanical response of an ecofriendly sawdust high strength concrete at elevated temperatures." Construction and Building Materials **258**: 119656.

Knaack, A. M., et al. (2011). "Compressive stress-strain relationships for North American concrete under elevated temperatures." ACI Materials Journal **108**(3): 270.

Kodur, V. (2000). Spalling in high strength concrete exposed to fire: concerns, causes, critical parameters and cures. Advanced Technology in Structural Engineering**:** 1-9.

Kodur, V. (2014). "Properties of concrete at elevated temperatures." International Scholarly Research Notices **2014**.

Kodur, V., et al. (2013). "An approach to account for tie configuration in predicting fire resistance of reinforced concrete columns." Engineering structures **56**: 1976-1985.

Lankard, D. R., et al. (1971). "Effects of moisture content on the structural properties of portland cement concrete exposed to temperatures up to 500F." Special Publication **25**: 59-102.

Lau, A. and M. Anson (2006). "Effect of high temperatures on high performance steel fibre reinforced concrete." Cement and Concrete Research **36**(9): 1698-1707.

Lertwattanaruk, P., et al. (2012). "Utilization of ground waste seashells in cement mortars for masonry and plastering." Journal of environmental management **111**: 133-141.

Lie, T. and V. Kodur (1996). "Thermal and mechanical properties of steel-fibre-reinforced concrete at elevated temperatures." Canadian Journal of Civil Engineering **23**(2): 511-517.

Lie, T. T. and J. Woollerton (1988). Fire resistance of reinforced concrete columns: test results, National Research Council Canada, Institute for Research in Construction.

Luo, X., et al. (2000). "Effect of heating and cooling regimes on residual strength and microstructure of normal strength and high-performance concrete." Cement and Concrete Research **30**(3): 379-383.

Marar, K., et al. (2001). "Relationship between impact energy and compression toughness energy of high-strength fiber-reinforced concrete." Materials letters **47**(4-5): 297-304.

Marara, K., et al. (2011). "Compression specific toughness of normal strength steel fiber reinforced concrete (NSSFRC) and high strength steel fiber reinforced concrete (HSSFRC)." Materials Research **14**: 239-247.

Martínez-García, C., et al. (2019). "Design and properties of cement coating with mussel shell fine aggregate." Construction and Building Materials **215**: 494-507.

Mazloom, M., et al. (2004). "Effect of silica fume on mechanical properties of high-strength concrete." Cement and Concrete Composites **26**(4): 347-357.

Menzel, C. A. (1943). Tests of the fire resistance and thermal properties of solid concrete slabs and their significance, National Emergency Training Center.

Miura, T. and I. Iwaki (2000). "Strength development of concrete incorporating high levels of ground granulated blast-furnace slag at low temperatures." Materials Journal **97**(1): 66-70.

Naceri, A. and M. C. Hamina (2009). "Use of waste brick as a partial replacement of cement in mortar." Waste management **29**(8): 2378-2384.

Nadeem, A., et al. (2014). "The performance of fly ash and metakaolin concrete at elevated temperatures." Construction and Building Materials **62**: 67-76.

Nassif, A., et al. (1999). "The effects of rapid cooling by water quenching on the stiffness properties of fire-damaged concrete." Magazine of Concrete Research **51**(4): 255-261.

Netinger, I., et al. (2011). "The effect of high temperatures on the mechanical properties of concrete made with different types of aggregates." Fire Safety Journal **46**(7): 425-430.

Nguyen, D. H., et al. (2017). "Durability of pervious concrete using crushed seashells." Construction and Building Materials **135**: 137-150.

Noumowé, A., et al. (2009). "Thermo-mechanical characteristics of concrete at elevated temperatures up to 310 C." Nuclear Engineering and Design **239**(3): 470-476.

Oktay, H., et al. (2015). "Mechanical and thermophysical properties of lightweight aggregate concretes." Construction and Building Materials **96**: 217-225.

Othuman, M. A. and Y. Wang (2011). "Elevated-temperature thermal properties of lightweight foamed concrete." Construction and Building Materials **25**(2): 705-716.

Panda, K. C., et al. (2020). "Effect of rice husk ash on mechanical properties of concrete containing crushed seashell as fine aggregate." Materials Today: Proceedings **32**: 838-843.

Panda, K. C., et al. (2020). Effect of Ground Granulated Blast Furnace Slag on the Properties of Sea Shell Concrete. IOP Conference Series: Materials Science and Engineering, IOP Publishing.

Pašalić, S., et al. (2012). "Pozzolanic mortars based on waste building materials for the restoration of historical buildings." Chemical Industry and Chemical Engineering Quarterly/CICEQ **18**(2): 147-154.

Peng, G.-F., et al. (2008). "Effect of thermal shock due to rapid cooling on residual mechanical properties of fiber concrete exposed to high temperatures." Construction and Building Materials **22**(5): 948-955.

Peng, G., et al. (2001). "Chemical kinetics of CSH decomposition in hardened cement paste subjected to elevated temperatures up to 800 C." Advances in cement research **13**(2): 47-52.

Phan, L. T. (2002). "High-strength concrete at high temperature-an overview." Proceedings of 6th international symposiumon utilization of high strength/high performance concrete, Leipzig, Germany: 501-518.

Phan, L. T. and N. J. Carino (1998). "Review of mechanical properties of HSC at elevated temperature." Journal of Materials in Civil Engineering **10**(1): 58-65.

Phan, L. T. and N. J. Carino (2001). "Mechanical properties of high-strength concrete at elevated temperatures."

Phan, L. T. and N. J. Carino (2002). "Effects of test conditions and mixture proportions on behavior of high-strength concrete exposed to high temperatures." ACI Materials Journal **99**(1): 54-66.

Phan, L. T., et al. (2001). "Effects of elevated temperature exposure on heating characteristics, spalling, and residual properties of high performance concrete." Materials and structures **34**(2): 83-91.

Phan, L. T. and L. Phan (1996). Fire performance of high-strength concrete: A report of the state-of-the art, US Department of Commerce, Technology Administration, National Institute of ….

Poon, C.-S., et al. (2001). "Comparison of the strength and durability performance of normal-and high-strength pozzolanic concretes at elevated temperatures." Cement and Concrete Research **31**(9): 1291-1300.

Poon, C.-S., et al. (2003). "Performance of metakaolin concrete at elevated temperatures." Cement and Concrete Composites **25**(1): 83-89.

Poon, C. S., et al. (2000). "A study on high strength concrete prepared with large volumes of low calcium fly ash." Cement and Concrete Research **30**(3): 447-455.

Poon, C. S., et al. (2004). "Compressive behavior of fiber reinforced high-performance concrete subjected to elevated temperatures." Cement and Concrete Research **34**(12): 2215-2222.

Real, S., et al. (2016). "Contribution of structural lightweight aggregate concrete to the reduction of thermal bridging effect in buildings." Construction and Building Materials **121**: 460-470.

Rizwan, S. A. (2006). "High-performance mortars and concrete using secondary raw materials."

Safi, B., et al. (2011). "Rheology and zeta potential of cement pastes containing calcined silt and ground granulated blast-furnace slag." Materiales de Construcción **61**(303): 353-370.

Safi, B., et al. (2013). "Effect of the heat curing on strength development of self-compacting mortars containing calcined silt of dams and Ground Brick Waste." Materials Research **16**: 1058-1064.

Safi, B., et al. (2013). "The use of plastic waste as fine aggregate in the self-compacting mortars: Effect on physical and mechanical properties." Construction and Building Materials **43**: 436-442.

Safi, B., et al. (2015). "The use of seashells as a fine aggregate (by sand substitution) in self-compacting mortar (SCM)." Construction and Building Materials **78**: 430-438.

Sakr, K. and E. El-Hakim (2005). "Effect of high temperature or fire on heavy weight concrete properties." Cement and Concrete Research **35**(3): 590-596.

Sancak, E., et al. (2008). "Effects of elevated temperature on compressive strength and weight loss of the light-weight concrete with silica fume and superplasticizer." Cement and Concrete Composites **30**(8): 715-721.

Sanjayan, G. and L. Stocks (1993). "Spalling of high-strength silica fume concrete in fire." Materials Journal **90**(2): 170-173.

Shi, C. and K. Zheng (2007). "A review on the use of waste glasses in the production of cement and concrete." Resources, conservation and recycling **52**(2): 234-247.

Sikora, P., et al. (2018). "The effects of Fe3O4 and Fe3O4/SiO2 nanoparticles on the mechanical properties of cement mortars exposed to elevated temperatures." Construction and Building Materials **182**: 441-450.

Standard, A. (2016). "Standard practice for making and curing concrete test specimens in the laboratory." ASTM International.

Toutanji, H., et al. (2004). "Effect of supplementary cementitious materials on the compressive strength and durability of short-term cured concrete." Cement and Concrete Research **34**(2): 311-319.

Varhen, C., et al. (2017). "Experimental investigation of Peruvian scallop used as fine aggregate in concrete." Construction and Building Materials **136**: 533-540.

Xiao, J., et al. (2016). "Effect of strain rate on compressive behaviour of high-strength concrete after exposure to elevated temperatures." Fire Safety Journal **83**: 25-37.

Yang, E.-I., et al. (2005). "Effect of oyster shell substituted for fine aggregate on concrete characteristics: Part I. Fundamental properties." Cement and Concrete Research **35**(11): 2175-2182.

Yu, Z. and D. Lau (2017). "Evaluation on mechanical enhancement and fire resistance of carbon nanotube (CNT) reinforced concrete." Coupled Syst. Mech **6**(3): 335-349.

Zeiml, M., et al. (2006). "How do polypropylene fibers improve the spalling behavior of in-situ concrete?" Cement and Concrete Research **36**(5): 929-942.